

FACULDADE DE ENGENHARIA DA UNIVERSIDADE DO PORTO



FEUP FACULDADE DE ENGENHARIA
UNIVERSIDADE DO PORTO

Therapeutic Applications of Electromagnetic Radiation

Modelling of Tissue Heating with ADS

Joana da Silva Gomes

Mestrado em Engenharia Biomédica

Supervisor: José Machado da Silva

Co-Supervisor: Luís Pessoa


July 27, 2016

A Dissertação intitulada


“Aplicações Terapêuticas da Radiação Eletromagnética”

foi aprovada em provas realizadas em 22-07-2016


o júri


Presidente Prof. Doutor Miguel Fernando Paiva Velhote Correia
Professor Auxiliar do Departamento de Engenharia Eletrotécnica e de Computadores da FEUP
- U.Porto


Prof. Doutor Rui Manuel Escadas Ramos Martins
Professor Auxiliar da Universidade de Aveiro


Prof. Doutor Jose Alberto Peixoto Machado da Silva
Professor Associado do Departamento de Engenharia Eletrotécnica e de Computadores da
FEUP - U. Porto

O autor declara que a presente dissertação (ou relatório de projeto) é da sua exclusiva autoria e foi escrita sem qualquer apoio externo não explicitamente autorizado. Os resultados, ideias, parágrafos, ou outros extratos tomados de ou inspirados em trabalhos de outros autores, e demais referências bibliográficas usadas, são corretamente citados.


Autor - Joana da Silva Gomes

Faculdade de Engenharia da Universidade do Porto

Therapeutic Applications of Electromagnetic Radiation

Modelling of Tissue Heating with ADS

Joana da Silva Gomes

Mestrado em Engenharia Biomédica

Faculdade de Engenharia da Universidade do Porto

July 27, 2016

Resumo

O presente trabalho de dissertação aborda o uso de radiação eletromagnética para fins terapêuticos. Começa com uma revisão sobre os campos eletromagnéticos e o seu uso em aplicações médicas. A fim de apresentar os conceitos fundamentais incluídos nesta tecnologia são descritos os pormenores sobre a modelação elétrica de tecidos, a propagação de radiação da fonte até ao recetor e como a modelação de propagação é aplicada para modelar a transferência de potência a partir de um emissor para o tumor, utilizando as propriedades dielétricas dos tecidos. Para este efeito, está a ser desenvolvido um modelo matemático cujo objetivo principal é determinar a frequência, a energia e o tempo necessário para garantir que no tumor é alcançada determinada temperatura. Para validar este modelo matemático, foram seguidas duas abordagens. Em primeiro lugar, o programa Advanced Design System destina-se a simular a temperatura dos diferentes tecidos e também o aumento de temperatura após o processo de aquecimento. Numa segunda fase, foram feitas algumas experiências para avaliar o processo de aquecimento por meio de um fantoma que imita um tumor de tecido mamário e uma câmara de infravermelhos, que é usada para medir a temperatura.

Abstract

The present dissertation work addresses the use of electromagnetic radiation for therapeutic purposes. It starts with a review on the electromagnetic fields and their use in medical applications. In order to present the fundamental concepts underlying this technology, details on the electrical modeling of tissues, the propagation of radiation from the source to the receptor and how propagation modelling is applied to model the transference of power from an emitter to the tumor using the dielectric properties of the tissues are described. For this purpose, a mathematical model whose main goal is to determine the frequency, power and the time needed to ensure that a certain temperature in the tumour is attained is being developed. To validate this mathematical model two approaches were followed. In first place, Advanced Design System program is meant to simulate the temperature of the different tissues and also the temperature rise after the heating process. In a second stage, some trials were made to evaluate the heating process by using a breast tumour emulating phantom and an infra-red camera monitoring system which is used to measure the temperature.

Acknowledgments

The implementation of this master was only possible due to a number of people that contributed, directly or indirectly, to the construction of this route and without which it would not be possible to reach the end.

Firstly, I would like to thank my thesis supervisor, Prof. José Machado da Silva, for his availability, his guidance and improvement suggestions about my research and writing. Also, to thank the knowledge that shared with me and the incentive to overcome the obstacles that appeared along the way and to achieve good results.

I would also like to thank Dr. Luís Pessoa and Dr. Mário Pereira who were involved in the validation survey for this research project and gave me much support to successfully conduct the validation experiments.

I acknowledge as well the contribution of Prof. Arminda Alves, Prof. Cidália Botelho and Eng. Liliana Pereira, for their support and availability in the preparation of the phantoms for the experimental work.

Finally, I must express my gratitude to my family, especially my parents, sister and godparents, and my friends for providing me with unfailing support, continuous encouragement and patience throughout my years of study and through the process of researching and writing this thesis. This accomplishment would not have been possible without them.

Joana da Silva Gomes

Contents

1	Introduction	1
1.1	Goals	1
1.2	Motivation	1
1.3	Dissertation Structure	2
2	Electromagnetic Radiation and Medical Applications	3
2.1	Electromagnetic Radiation	3
2.1.1	Electromagnetic Waves and Electromagnetic Fields	3
2.1.2	Electromagnetic Fields and Biological Tissues	6
2.1.3	Effects of Electromagnetic Radiation on Health	10
2.1.4	Exposure Guidelines to Electromagnetic Fields	11
2.2	Examples of Electromagnetic Radiation Based Therapeutic Approaches	13
2.2.1	Microwave Based Therapeutic Approaches	13
2.2.2	Radio-frequency Based Therapeutic Approaches	16
2.2.3	Comparison Between Microwave Ablation and Radio-frequency Ablation	21
2.3	Radio-frequency Circuits	22
2.3.1	Power Amplifiers	22
2.3.2	Impedance Matching	23
2.3.3	Antennas	24
2.4	Conclusions	25
3	An Electrical Model of Tissue Heating	27
3.1	Electrical RC Model of Biological Tissue	29
3.2	Electrical Model Based on Electromagnetic Propagation	31
3.3	Thermal Models With Heat Dissipation	33
3.3.1	Stationary Thermal Model	34
3.3.2	Transient Thermal Model	34
3.4	Experimental	35
3.5	Conclusions	38
4	Tissue Heating Simulation and Experimental Results	39
4.1	Simulations Results	39
4.1.1	Electric Model Based on Electromagnetic Propagation	39
4.1.2	Thermal Models With Heat Dissipation	41
4.2	Experimental Results	45
4.3	Conclusions	47

5	Conclusions and Future Work	49
5.1	Future Work	49
	References	51

List of Figures

2.1	The electromagnetic spectrum [[1]].	5
2.2	Types of biological tissues [2].	7
2.3	Representation of the induction heating generated by the magnetic field [3].	9
2.4	Representation of the conformal antenna used [4].	14
2.5	Block diagram of a simplified RF transmitter [5].	22
2.6	Block diagram of a simplified RF receiver [5].	23
3.1	RC equivalent model of each tissue.	29
3.2	Representation of the electric circuit model used in the ADS.	31
3.3	Representation of the set of variables used in the electric circuit model.	32
3.4	Representation of the transmission matrix.	32
3.5	Representation of the scattering matrix.	32
3.6	Thermal model with heat dissipation used in the ADS that simulates the temperature of the tumour.	34
3.7	Transient thermal model with heat dissipation used in the ADS that simulates the behaviour of temperature through time.	35
3.8	Phantom material that represents breast tumour.	36
3.9	Scheme of the experimental setup used in the heating of the phantom.	37
3.10	Power source used in the experimental setup of the phantom heating.	37
3.11	Amplifier used in the experimental setup of the phantom heating.	37
3.12	Antenna, phantom and camera used in the experimental setup of the phantom heating.	38
4.1	Representation of the power dissipated in each tissue as function of frequency.	40
4.2	Representation of the electric conductivity in the tissues as function of frequency.	40
4.3	Temperature of the three layers of breast tissue at the different frequencies, for the thermal model with heat dissipation.	42
4.4	Variation of temperature through time for a frequency of 433 MHz.	43
4.5	Variation of temperature through time for a frequency of 915 MHz.	44
4.6	Variation of temperature with time for a frequency of 2 GHz.	44
4.7	Variation of temperature with time for the different frequencies.	45
4.8	Phantom at the beginning of the exposure time.	46
4.9	Phantom at the end of the exposure time.	46
4.10	Acrylic plate at the beginning of the exposure time.	46
4.11	Acrylic plate at the end of the exposure time.	47

List of Tables

2.1	Electromagnetic radiation basic restrictions.	12
2.2	Reference levels.	13
3.1	Dielectric properties of each tissue for the different frequencies used in the simulated models [6].	33
3.2	Composition of breast tumour phantom.	36
4.1	Power dissipated in each tissue and voltage observed in the tumour for the different frequencies.	41

Abbreviations and Symbols

List of abbreviations (sort by alphabetical order)

AC	Alternate Current
ADS	Advanced Design System
CT	Computed Tomography
EM	Electromagnetic
EMT	Electromagnetic Thermotherapy
FDTD	Finite Difference Time Domain
FEUP	Faculdade de Engenharia da Universidade do Porto
LC	Inductance and capacitance parallel circuit
MOM	Method of Moments
PET	Positron Emission Tomography
RF	Radio Frequency
SAR	Specific Absorption Rate
VSWR	Voltage Standing Wave Ratio
EIRP	Equivalent Isotropic Radiated Power

List of symbols

v	Velocity of propagation
f	Frequency
λ	Wavelength
c	Velocity of light
γ	Propagation constant
α	Attenuation constant
β	Phase constant
d	Depth of penetration
ω	Angular frequency
μ	Magnetic permeability
E	Electric field strength
ϵ	Permittivity
$\tan \delta$	Loss tangent
σ	Electric conductivity
ρ	Density
ϵ''	Loss factor
ϵ'	Relative permittivity
C_p	Specific Heat
k	Thermal Conductivity
C	Thermal Capacity
R_{th}	Thermal Resistivity
ΔQ	Thermal Energy

Chapter 1

Introduction

1.1 Goals

The work presented in this dissertation aims at studying the effects of electromagnetic radiation in the human body and its use for medical purposes. From a biological point of view, it is intended to study the radiation effects in a frequency spread spectrum, namely in the non-ionizing radiation which includes the radio-frequency and microwave energies. In addition, and as the main contribution, this work also aims to study the heating of human tissues by means of electromagnetic radiation, as well as the electrical modelling of the propagation path from the radiation emitter to the targeted tissue, notably a tumour, using ADS, and how this propagation model is applied using the dielectric properties of the tissues. The discussion of the effects of electromagnetic radiation can be also done in other simulators such as HFSS (High Frequency Structural Simulator), COMSOL or Sim4Life which are 3-D simulators. However, these simulators are much slower once imply more memory and computer time so the proposed modelling in ADS allows faster simulations and the simulation of all system, from signal generation to heat dissipation.

1.2 Motivation

Radio-frequency (RF) electromagnetic radiation has been explored as a therapeutic means to treat cancer and other diseases, such as hyperthermia for treating tumours, or even to be used for microwave imaging as an alternative to the X-ray imaging technique.

Given the continuous increase of cancer diseases and the high costs involved in their treatment, RF based treatment approaches are becoming relevant. That is the case with hyperthermia treatment, which is the heating of tissues to approximately 40-42 °C, or even ablation, which is the heating of the targeted tissue with a temperature around 60°C, can be considered the most suitable therapy for certain cases, such as inoperable cancers and for high-risk surgical patients. In addition, this work contributes to the use of alternative techniques whose effects upon biological tissues can be beneficial and used for medical purposes.

However, the main challenge is to achieve a treatment whose heating process is controlled and localised.

1.3 Dissertation Structure

In first place, in chapter 2, a bibliographic revision is presented on subjects related to electromagnetic radiation and medical applications. This chapter is divided in three sections: electromagnetic radiation, examples of electromagnetic radiation based therapeutic approaches, and radio-frequency circuits. The first section addresses electromagnetic waves and electromagnetic fields, their relation with biological tissues, the effects of electromagnetic radiation on health and exposure guidelines to electromagnetic fields. The second section presents microwave and radio-frequency based therapeutic approaches and the comparison between microwave and radio-frequency ablation methods. The last section refers to material and concepts that are used in radio-frequency circuits, such as power amplifiers, impedance matching and antennas.

In chapter 3, the different modelling approaches studied here are described. The methodology of the dissertation work is presented and can be separated in electrical model based on mathematics and based on electromagnetic propagation, thermal model with heat dissipation, transient thermal model with heat dissipation and experimental. The first four sections addresses to simulations performed in Advanced Design System program with the main goal of studying the heating of tissues. On the other hand, in experimental the heating of tissues is also analysed by using a phantom that mimics breast tumour tissue and whose temperature is measured by an infrared camera.

Chapter 4 is dedicated to, first, present the results of the simulations carried out in Advanced Design System program after applying different frequencies. Experimental results obtained by applying electromagnetic radiation to a breast tumour emulating phantom are presented which allowed to verify some of the conclusions obtained from the simulations.

The last chapter, 5, is the discussion of the simulation and experimental results, the comparison between them and some future perspectives of work that can be made to improve the results.

Chapter 2

Electromagnetic Radiation and Medical Applications

2.1 Electromagnetic Radiation

2.1.1 Electromagnetic Waves and Electromagnetic Fields

Electromagnetic (EM) fields are physical fields produced after a combination of electric and magnetic fields. The first are produced by stationary charges and the second by moving charges. EM fields propagate indefinitely throughout space in a wavelike manner, whose amplitude declines with the distance from the EM source in a manner which depends on the propagation medium. The velocity of propagation v of the generated EM field is proportional to the frequency f (in Hertz, Hz) and the length λ (in meters, m) of the wave, according to $v = f \times \lambda$. It varies with the propagation medium, being equal to the velocity of light, c (approximately $3,00 \times 10^8$ m/s in the vacuum). When a wave propagates through different media its velocity changes but its frequency remains constant — this means that the wavelength changes according $\lambda = \frac{\lambda_0}{n(\lambda_0)}$ where $n(\lambda_0)$ is the refractive index of the medium at wavelength λ_0 [7].

The propagation mechanisms of EM fields govern the processes that determine how EM fields behave at the boundary between two media, which include wave reflection, transmission/refraction, diffraction and scattering.

Wave reflection and refraction are linked to each other once, normally, when an electromagnetic wave reaches a boundary between two media, it is partially reflected back and partially refracted [8]. The reflection coefficient is the ratio of the reflected wave to the incident wave or, as expressed in equation 2.2, the ratio between the reflected power and the incident power which is expressed in dB.

$$\Gamma = 10 \times \log\left(\frac{P_r}{P_i}\right) \quad (2.1)$$

The transmission coefficient is defined as the ratio of the transmitted wave to the incident wave. However, to obtain these parameters it is necessary to use the field approach, which implies the

definition of the boundary conditions, which is a complicated process. The angle of refraction of an electric field between two media depends on the permittivity (ϵ) of each medium, i. e., $\frac{\tan\theta_1}{\tan\theta_2} = \frac{\epsilon_2}{\epsilon_1}$, and the angle of refraction of a magnetic field between two media on the permeability (μ) of each medium, i. e., $\frac{\tan\theta_1}{\tan\theta_2} = \frac{\mu_2}{\mu_1}$.

Alternatively, the equivalent electric circuit approach can be used, where the two media are replaced by two analogous transmission lines with characteristic impedances that are determined by wave polarization, incident angle and material properties.

On the other hand, diffraction is considered the apparent bending and spreading of waves when they encounter an obstacle. Scattering occurs when the obstacle dimensions are similar or smaller than the wavelength and consists in the diffusion of a portion of the incident wave in all directions [8].

Emittance and emissivity are parameters used to characterize the source of EM fields. The emittance defines the energy radiated by a surface. If a surface does not emit the same in all directions it can be considered a directional emittance whose maximum emission occurs in the normal direction to the radiating surface. Emissivity is a material property that measures the ability of a surface to emit energy under certain conditions [4].

When electromagnetic propagation mechanisms are addressed, it is necessary to take into account that propagation and attenuation occur. The propagation constant can be calculated by the next equation:

$$\gamma = \alpha + j\beta, \quad (2.2)$$

where the real part, α , is the attenuation constant and the imaginary part, β , is denominated as phase constant. In addition, the attenuation constant and the phase constant are determined by the following equations:

$$\alpha = \omega \cdot \sqrt{\mu \cdot \epsilon} \cdot \left[\frac{1}{2} \cdot (\sqrt{1 + \tan^2 \delta} - 1) \right]^{\frac{1}{2}} \quad (2.3)$$

and

$$\beta = \omega \cdot \sqrt{\mu \cdot \epsilon} \cdot \left[\frac{1}{2} \cdot (\sqrt{1 + \tan^2 \delta} + 1) \right]^{\frac{1}{2}} \quad (2.4)$$

where ω is the angular frequency, μ is the magnetic permeability, ϵ is the permittivity and $\tan \delta$ is the loss tangent. The depth of penetration (d) is defined as the distance at which the amplitude of the electromagnetic fields is attenuated by a value of 1 Neper and is defined by the following equation:

$$d = \frac{1}{\alpha} = \sqrt{\frac{2}{\omega \mu \sigma}} \quad (2.5)$$

where σ is the electric conductivity. Therefore, it is possible to achieve that the attenuation increases with frequency while the depth of penetration diminishes as frequency rises and that they are inversely proportional to each other.

EM are present in a wide variety of forms in the environment, generated by both natural and

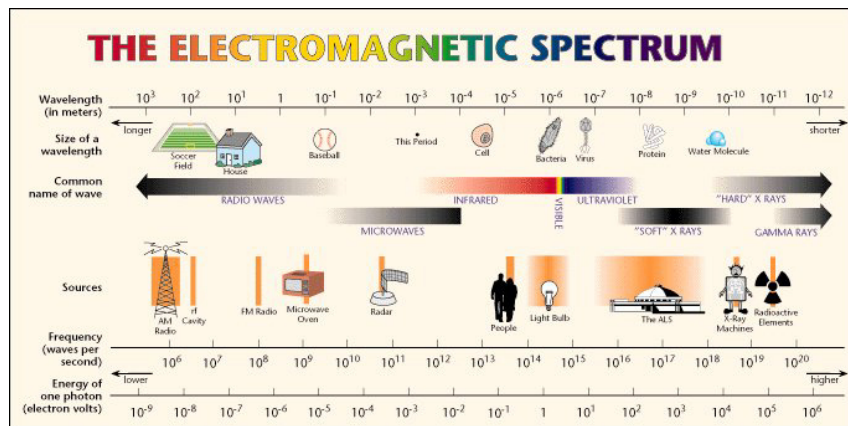


Figure 2.1: The electromagnetic spectrum [[1]].

human-made sources. Among the first ones one have, for example, the earth's magnetic field and as examples of human-made sources one can mention the x-rays and the waves used in radio systems.

The types of EM fields can be divided in three groups, low-frequency, intermediate-frequency and high-frequency fields, corresponding, respectively, to the ranges up to 300 Hz, from 300 Hz to 10 MHz and from 10 MHz to 300 GHz. Concerning the subject of this work, the most important fields are high-frequency or radio-frequency fields found in the range from 10 MHz to 300 GHz. These can be produced by radio transmitters or mobile phones and are commonly used to transmit information at long distances [9]. Figure 2.1 shows the electromagnetic spectrum in which it is possible to observe the different applications for radiation and the respective frequency.

The electric and magnetic fields of an electromagnetic wave are aligned with planes that are at right angles to one another and to the direction of the motion of the wave. These fields are linked to each other once, at any time an electric field changes it creates a magnetic field that is generated by the electric field current, which leads to the fact that magnetic fields are only produced once an electric current changes. The electric field (E) is defined as the force per unit charge and it is expressed in V/m. From this field it is possible to determine the electric flux density D , i.e., a measure of how much electric flux passes through a unit area, by the product between the electric permittivity and the electric field:

$$D = \epsilon.E \quad (2.6)$$

The electric field is also used to calculate the current density J (in A/m²) by the product between the electric field and electric conductivity:

$$J = \sigma.E \quad (2.7)$$

Similarly, a magnetic field (H), expressed in A/m, has greater intensity close to the origin and rapidly decreases with the increasing distance from the source. The magnetic flux density is

obtained by the product between the magnetic permeability and the magnetic field:

$$B = \mu.H \quad (2.8)$$

2.1.2 Electromagnetic Fields and Biological Tissues

EM waves transport energy, momentum and angular momentum and thus affect the behaviour of matter in its vicinity. Regarding their interaction with biological tissues they can be classified in ionizing and non-ionizing radiations according to the effects that can be provoked, because fields of different frequencies interact with the body in different ways. Ionizing radiation occurs when the electromagnetic radiation is capable of causing the removal of an electron from an atom or molecule, i.e., when the energy of each photon is greater than the binding energy of the electrons, which can origin free radicals which, in turn, increase the risk of chromosomal anomalies. Ionizing radiation presents frequencies above the visible spectrum, i.e., above a frequency of 10^{15} Hz. Non-ionizing radiation is characterised by the fact that it conveys energy only to excite the motion of the atoms or molecules or to move an electron from an occupied orbital into an empty higher energy orbital. Anyway, these can cause effects such as thermal effects and include radio-frequencies in the range from 3 kHz to 300 MHz and microwaves whose frequency range is from 300 MHz to 300 GHz [7].

The propagation of an electromagnetic field through a biological tissue can be expressed resorting to Maxwell's equations, i.e., four equations which relate the electric and magnetic fields with electric charge and electric current [8].

$$\nabla \cdot \vec{D} = \rho \quad (2.9)$$

$$\nabla \cdot \vec{B} = 0 \quad (2.10)$$

$$\nabla \times \vec{E} = -j\omega\vec{B} \quad (2.11)$$

$$\nabla \times \vec{H} = \vec{J} + \vec{J}_s + j\omega\vec{D} \quad (2.12)$$

where \vec{D} is the electric flux density, \vec{E} is the electric field, \vec{B} is the magnetic flux density, \vec{H} is the magnetic field, ρ is the charge density, \vec{J} is the current density and \vec{J}_s is the added source current density on the antenna [10].

The human body biological tissues can be divided in four groups: epithelial, connective, muscle and nervous tissues, as represented in picture 2.2.

The epithelial tissues cover all body surfaces both inside and out and their functions include protection, sensory perception and secretion. The connective tissues, such as the adipose tissue, are considered the most abundant ones in the body and are responsible for providing support, protection and for storing fat. The muscle tissues are present in skeletal muscles, in hollow organs

Human Body Tissues

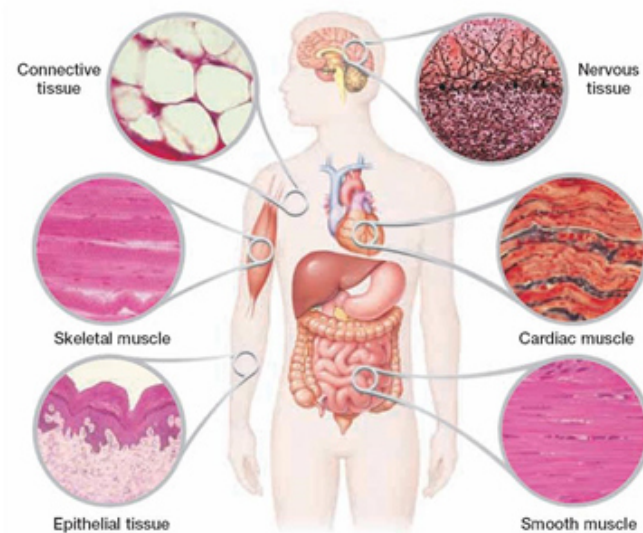


Figure 2.2: Types of biological tissues [2].

and in cardiac muscles and are responsible for the contraction of these muscles. The nervous tissues react to stimuli and conduct electrical impulses through the body to target organs and can be found in brain, spinal cord and nerves.

In order to study the interaction between the electromagnetic fields and biological tissues it is necessary to be acquainted with the dielectric properties of the biological tissues subject to the radiation. The dielectric properties of the tissues, the electric conductivity (σ), the electric permittivity (ϵ) and the magnetic permeability (μ), are specific for each type of tissue and influenced by some factors, for example, the frequency and temperature.

The measurable parameters are the electric conductivity and the electric permittivity that are capable of providing information about the structure and composition of the biological tissues, such as the fat content, or the presence of a tumour. Besides, these properties depend also upon the water content, once as the water presented in a tissue increases the electric conductivity also increases [7].

To study the interaction between the electromagnetic fields and biological tissues, phantom materials that mimic the behaviour of biological tissues, can be done. Phantom materials provide an approximate emulation of the electromagnetic properties on human body over a determined frequency and temperature range. Due to that fact, it is impossible to develop one phantom material to simulate tissue at all frequencies, because the different dielectric relaxation phenomena depend on tissue cell membrane and certain ionic properties [11],[12]. Another definition for a phantom is a material that provides a simulation of a biological body or a physical model which shows properties similar to those of a biological tissue.

The use of phantom materials in the context of using RF energy for therapeutic purposes, is to study the interaction between the human body tissues and the electromagnetic fields, in order to evaluate how, e. g., the electrical characteristics of the body affect the design of the power stage of communication devices placed within the human body [12] or to evaluate potential heating effects.

The phantom materials can be classified, most commonly, from three different points of view. In first place, there is the frequency criterion which divides the phantom materials in two groups, i.e., materials that work in the low frequency and others that work in the high frequency range. Another criterion is the type of biological tissue which divides the phantom materials, also, in two groups such as a group of tissues containing much water like muscle, brain and internal organs and, on the other hand, the group of tissues that contain as little water as bone and fat. Lastly, the most common classification criterion is based on the final state of the material and can be divided in three groups, solid (dry), solid (gel) and liquid [12].

In addition, phantoms can be considered static or dynamic. Static phantoms are useful for the determination of specific absorption rate patterns, i.e., heating pattern, assuming no heat loss. On the opposite side, dynamic phantoms are more useful for simulation of patient treatment due to the more realistic thermal properties and blood perfusion [11].

Another aspect of the phantom materials is that they are specifically employed for experimental use, resulting in physical characteristics such as body shape, electrical and magnetic constants and temperature, due to the fact that the human body is electrically heterogeneous. However, in order to the phantom materials be suitable for tissue heating applications, the dielectric properties of the phantom model must closely approximate those of the tissue over the temperature range of interest. Concerning tumours, the phantom materials used to simulate their behaviours are more difficult to achieve, because tumours have a wide range of dielectric properties comparatively with normal tissues [11],[12].

For the development of the phantom, due to the fact that the dielectric properties of the phantom must be similar to those of the tissue in study as referred above, it is necessary to consider the relative permittivity and the conductivity. With respect to the relative permittivity of dielectric materials, its value can be regulated by the use of typical materials such as glycerol. On the other hand, for a known and controlled conductivity, a saline solution, normally of sodium chloride in deionized water, is used to regulate its value by varying the salt concentration [12].

One exception in the development of the phantom, is when the phantom material is in a liquid state that involves the addition of a substance with gelatinous elements, for example agar, in order to increase the solidity of the solution without changing the linear relationship between the conductivity and salt concentration, allowing the sample to have greater stiffness and malleability which allows for the physical model to be made. Though the distribution of the agar in the phantom must be homogeneous to ensure uniform conductivity in the entire volume. In addition, the agar has the same variation in temperature comparatively to the phantom without this substance [12].

The phantom tissue has a limited useful life time, i.e., takes, approximately, two weeks before deterioration becomes apparent and the material turns into soup and the escape of fluid occurs,

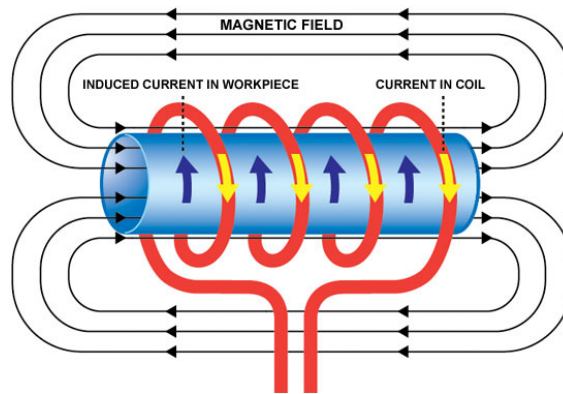


Figure 2.3: Representation of the induction heating generated by the magnetic field [3].

changing the dielectric properties of the phantom. However, the lifetime of the phantom can be prolonged by refrigeration [11].

Another important aspect in the development of phantoms is the selection of frequencies used. The frequencies most commonly used, for medical applications, are 13.56 MHz, 27.12 MHz, 433 MHz and 915 MHz, because they are authorized industrial, scientific and medical bands [11].

Due to the technological advances that have been observed in the development of biocompatible materials, bioimplantes capable of sensing a physiological parameter and transmit it via a radio-frequency link to an external receiver for analysis or diagnosis are now common. Resorting to tissue substitute materials, suitable to reproducing the attenuation of electromagnetic energy in the same way as the different tissues of the human body, the data transmission process can be studied in more detail.

An electromagnetic field has some unexplained effects on human body, but one of them has been proved, the thermal effect which is caused by electromagnetic fields of high frequencies.

In this process, there is a radio-frequency power supply used to drive a large alternating current through an inductor or antenna, which generates a very intense and rapidly changing electromagnetic field. Under radiation the tissue behaves as an electrical circuit, resulting in the production of circulating eddy currents. An alternating currents passing in the tissues cause ions to vibrate in an attempt to follow the change in the direction of the rapidly alternating current. It is the ionic friction that generates precise and localized heating, also denominated as “Joule effect”, in the tissue. The current density is $\vec{J} = \sigma \times \vec{E}$. The higher the current, the more intense the motion of the ions and the higher the temperature reached over a certain time, eventually leading to necrosis and cell death. In the figure 2.3 it is possible to observe how the magnetic field generates the heat by the presence of the induced currents and the “Joule effect”.

This type of electromagnetic fields, which are generated on the surface or in the depth of biological tissue, can be observed by three methods, measurement with infra-red cameras, measurement with special phantoms of biological tissue and measurement with water phantoms. The first technique, with a thermovision camera, is divided in three parts: (1) the person’s temperature is measured before the exposure to electromagnetic fields, (2) measurements are made with

for example a mobile phone during a call and, (3) the subject under evaluation is measured when the telephone call is finished but after the time exposure, which is defined at the beginning of the process, for example ten minutes. For this method, is necessary to consider the spacing between person's ear and the device, but it is possible to conclude that the temperature of person's ear is higher after telephone call than before.

Other techniques can be applied for calculating the temperature rising related to direct absorption of electromagnetic energy [13]. Usually, for this type of numerical calculations of the electromagnetic energy absorption, i.e., in order to calculate the specific absorption rate (SAR) two methods are used, the Method of Moments (MOM), which is a frequency domain technique, or the Finite Difference Time Domain (FDTD), which is a time domain method [14]. However, the method most often used is the FDTD. The FDTD method is one of the most adequate for computing electromagnetic fields and it is more efficient in terms of computer time and memory, comparatively to other methods, because there is no matrix to fill and solve. Besides, it provides results for a wide spectrum of frequencies from only one calculation using transient pulse excitation and fast Fourier transformation and is based on a solution grid which is composed by rectangular boxes and each box edge is an electrical field location [13].

Another aspect to be considered in this method, is the fact that, for study purposes, it is safer than resorting to measurements done by exposing people to electromagnetic fields, because it only simulates the exposure, so a diagnostic person is not necessary.

As mentioned before, the FDTD method is used to calculate the specific absorption rate in order to analyse the electromagnetic energy absorbed by human tissues. With respect to the specific absorption rate distribution, the region with maximum field corresponds to the region with the greater value of specific absorption rate. In addition, for this type of calculations, the body organs under research are modelled in such a way that calculations can be done in a simple way, for example for the eye and the brain, a spherical and rectangular model are used, respectively [14].

2.1.3 Effects of Electromagnetic Radiation on Health

Regarding the effects on health, nowadays there is no relevant scientific evidence indicating adverse health and biological effects as a result of radio-frequency exposure at levels below national and international safety standards. However, this fact does not ensure that exposure to weak electromagnetic fields is harmless to human body [15].

It is known that the exposure to high levels of radio-frequency radiation can be harmful due to, in first place, the increase of body temperature. This can lead to tissue damage due to the body's inability to dissipate the excessive heat that could be generated, namely in areas with relative lack of available blood flow. The extent of heating of the biological tissue depends on several factors such as radiation frequency, size, shape and orientation of the exposed object, exposure time and efficiency of heat dissipation.

Another possible effect from exposure to radio-frequency fields in the range up to 10 MHz is the excitation of nerve tissues that can occur when electric fields are induced above certain intensities in the body [16].

In order to achieve consensus about the effects of the exposure to radiation, many health effects have been studied, such as the risk of cancer development, the effects on reproduction, gene expression in cells, effects on the body systems and electromagnetic hypersensitivity. Regarding the risk of cancer development, the studies that have been developed show evidence that exposure to weak radio-frequency fields does not lead to cancer.

As far as reproduction and thermal effects are concerned, it is known that exposure to radio-frequency fields can damage sperm. From the studies of sperm samples from humans and animals that have been carried out, it is not possible to draw conclusions about possible non-thermal effects of radio-frequency exposure on sperm. However, from the current studies there is little indication that exposure to weak radio-frequency fields affects fertility.

Regarding gene expression in cells, studies have been made to observe changes in gene expression after radio-frequency exposure, but the obtained results are inconsistent. So there is no evidence that exposure to weak radio-frequency fields leads to changes in gene expression capable of causing adverse effects in the human body.

Concerning the human body, the studies that have been done indicate no evidence between possible non-thermal effects, namely biological effects, and exposure to weak radio-frequency fields.

Electromagnetic hypersensitivity indicates a condition where individuals believe that their health problems are caused by EM fields. The current literature provides no evidence that exposure to EM fields may affect the onset of symptoms. Therefore, it is possible to deduce that the health problems attributed to EM fields are caused by other influences such as stress reactions, cultural conditions, and other psychological mechanisms [16].

2.1.4 Exposure Guidelines to Electromagnetic Fields

The EM fields are present regularly in our daily life, once with the development of industry the exposure to them has increased substantially. Therefore, it is necessary to determine the level of exposure to which humans can be subject to. These can be divided in two categories: base restrictions and reference levels. The base restrictions are derived from the exposure threshold values according to the health effects and other factors such as the work. In order to establish these restrictions, the physical quantities used are the field frequency, magnetic flux density, current density, power density, and the specific absorption rate (SAR) that is calculated by the following equation:

$$SAR = \frac{\sigma \cdot |E|^2}{2\rho}, \quad (2.13)$$

where E is the peak electric field strength¹, σ the tissue conductivity in S/m, and ρ is the tissue

¹The division by 2 is needed to obtain RMS values, considering sinusoidal waves.

Table 2.1: Electromagnetic radiation basic restrictions.

Frequency Range (Hz)	Magnetic Flux Density, B (mT)	Current Density, J (mA/m ²)	Average SAR for whole body (W/kg)	Localised SAR (head and trunk) (W/kg)	Localised SAR (members) (W/kg)	Power density, S (W/m ²)
0	40	-	-	-	-	-
>0-1	-	8	-	-	-	-
1-4	-	8/f	-	-	-	-
4-1000	-	2	-	-	-	-
1000-100k	-	f/500	-	-	-	-
100k-10M	-	f/500	0.08	2	4	-
10M-10G	-	-	0.08	2	4	-
10G-300G	-	-	-	-	-	10

density in kg/m³. SAR measures the rate at which energy is absorbed by the human body when exposed to a radio-frequency field and is expressed in W/kg. It represents the average power deposited per unit mass of tissue at any position.

For workers and general public, the basic restrictions values are, respectively, $\frac{1}{100}$ and $\frac{1}{50}$ of the exposure threshold value of 4 W/kg for the specific absorption rate [16]. From the base restrictions levels, it is possible to obtain the reference values which are derived from the external fields, i.e., the values that can be measured in the air outside the body, and are used as evaluation methods with the objective of determining if the base restrictions are exceeded during exposure [7], [16]. The basic restrictions and the reference levels for the general public are represented in tables 2.1 and 2.2.

From table 2.1 it is possible to verify that, for the frequency range of interest to this work, the basic restrictions are related, mainly, to the specific absorption rate limits.

Table 2.2 shows the effective values that correspond to the relevant basic restrictions. From this table, it can be verified that to evaluate the exposure level of radiation, which is characterised by SAR, it is only necessary to measure the intensity field and the power density to obtain the specific absorption rate.

The exposure guidelines present the evaluation of the risk of radiation exposure, the risk assessment, as an analytical tool for characterising possible health risks to individuals or populations through combining existing epidemiological and lab data on the potency of an agent with estimates of expected levels of human exposure. A complete risk assessment comprises hazard identification, exposure assessment, exposure-response evaluation and risk characterisation. Hazard identification refers to reach a conclusion about if exposure to an agent can provoke an increase in the incidence of certain health condition. Exposure assessment is the characterisation of the spatial and temporal patterns of exposure to the agent. Exposure-response evaluation addresses to collecting, from epidemiological studies and laboratory data, a relation between the level of exposure and the magnitude of the induced health hazard. Risk characterisation involves the combination between estimates of exposure and estimates of effect per unit of exposure in order to obtain quantitative statements about human health risk.

On the other hand, the risk assessment process has some uncertainties, such as the fact that an agent induces adverse effects at high exposure levels, but that can be harmless or even beneficial

Table 2.2: Reference levels.

Frequency Range (Hz)	Field intensity, E (V/m)	Field intensity, H (A/m)	Field intensity, B (microT)	Equivalent power density of a plane wave, S_{eq} (W/m ²)
0-1	-	3.2×10^4	4×10^4	-
1-8	10000	$3.2 \times 10^4 / f^2$	$4 \times 10^4 / f^2$	-
8-25	10000	$4000/f$	$5000/f$	-
0.025k-0.8k	$250/f$	$4/f$	$5/f$	-
0.8k-3k	$250/f$	5	6.25	-
3k-150k	87	5	6.25	-
0.15M-1M	87	$0.73/f$	$0.92/f$	-
1M-10M	$87/f^{1/2}$	$0.73/f$	$0.92/f$	-
10M-400M	28	0.073	0.092	2
400M-2000M	$1.375f^{1/2}$	$0.0037f^{1/2}$	$0.0046f^{1/2}$	$f/200$
2G-300G	61	0.16	0.20	10

at very low exposure levels. The lack of literature in laboratory data in humans is another source of uncertainty [17].

2.2 Examples of Electromagnetic Radiation Based Therapeutic Approaches

Concerning the application of electromagnetic radiation for therapeutic purposes, it is possible to separate them in two groups according to the frequency range, microwave and radio-frequency based therapeutic approaches.

2.2.1 Microwave Based Therapeutic Approaches

2.2.1.1 Microwave imaging

One example of the use of EM radiation for therapeutic purposes is microwave imaging for breast cancer detection, which can be considered a safer alternative to the current X-ray imaging technique. In this technique, in order to distinguish breast tumours from normal tissues, the permittivities of both are compared because breast tumours have a higher permittivity contrast that causes strong reflection of the incident electromagnetic radiation.

With the aim of testing this microwave imaging system, in [4] a phantom that represents fatty breast tissues and a metallic sphere as a test target were used. This setup was radiated using frequencies in the range from 2 GHz to 5 GHz being a conformal antenna placed in many different positions in order to perform frequency response measurements to which the Kirchhoff Migration algorithm was applied to detect the target.



Figure 2.4: Representation of the conformal antenna used [4].

In the Kirchhoff Migration algorithm, if the distance of the scan point to the antenna is equal to the distance of the target, the electric field is maximum and a positive detection of the target is considered. On the other hand, if the distance of the scan point is different from the distance of the target, no target is detected. Usually this algorithm is applied using an antenna array where the antennas are geometrically separated from each other. However, in this particular case, it was necessary to design a conformal antenna, which is an antenna designed to conform or follow some prescribed shape, due to the curved surface of the flask, as shown in figure 2.4.

At each position the antenna input reflection coefficient was measured, which relates the energy reflection on the antenna itself, as well as the energy reflected by the target, so it is necessary to realise a calibration measurement without the target in order to eliminate the influence of the antenna caused by impedance mismatch.

Through the captured data, it was possible to observe that the measured input reflection coefficient was slightly higher compared to the simulations, once the dielectric properties measured with wet sand and distilled water were also superior. After applying the Kirchhoff Migration algorithm to the measured data, the results were found satisfactory once the metallic sphere was successfully detected despite some unwanted artifacts.

Lastly, this method does not present any known health hazard once its main effect is the slight increase of tissue temperature, but as main disadvantage one has a low resolution in exchange for penetration depth of the energy in the body [4].

2.2.1.2 Microwave Ablation

Electromagnetic radiation can also be found in thermotherapy systems in order to produce a fast and local heating of the targeted tissue to cause necrosis of tumour cells, i. e., a temperature above 60 °C.

Microwave ablation consists in dielectric heating, which occurs when an alternating electromagnetic field is applied to a tissue that acts as the dielectric material. When an electric charge from a radiating field oscillates, it interacts with a water molecule causing the molecule to flip. Microwave radiation is specially tuned to the natural frequency of water molecules to maximize this interaction. The heating occurs due to the fact that the electromagnetic field forces the tissue's water molecules to oscillate out of phase, resulting in the absorption of electromagnetic energy

and posterior conversion to heat [18]. The agitation of the water molecules in the surrounding tissue, produce friction and heat, leading to cellular death via coagulation necrosis [19].

Microwave ablation uses a frequency range from 300 MHz to 300 GHz. This procedure can be performed using a single microwave antenna or a configuration of more antennas to create a greater ablation volume, depending on the tumour size, and a 915 MHz generator or 2450 MHz generator.

It has been reported that thermal damage to cells begins at 42 °C and that above 60 °C, intra-cellular proteins are denatured, the lipid bilayer melts, and irreversible cell death occurs [20].

The method presented in [21] addresses the treatment of hyperhidrosis, which is a condition of excessive sweating and the aim of this method is ablation of the sweat glands that lie in close proximity to the boundary between the skin and fat layer, but to do it non-invasively and with minimal patient recovery time.

This technique can be divided in two approaches according to the frequency range. In the first case, with a high kHz to low MHz range, the radio-frequency current is conducted through tissue between an electrode and a ground plane or between two electrodes, resulting in the tissue's resistance to the flow of current generating Joule losses that lead to tissue heating. The second approach, using frequencies in the mid MHz range, has a similar procedure but uses capacitively or inductively radio-frequency applicators capable of inducing dielectric heating. However, these two radio-frequency approaches have as main disadvantage the local intense heating at the electrode edges which causes difficulty in efficient heating at a depth in the tissue while protecting the skin surface.

The microwave approach provides some inherent advantages such as the fact that in the microwave frequency range, the skin and fat tissues have very different dielectric properties which leads to a greater reflection at the skin/fat interface and, in turn, to the generation of a standing wave pattern in the skin.

Regarding the procedure, in a first stage a theoretical optimal frequency of 6,9 GHz is determined. At this theoretical frequency, the absorption level is at its maximum at the skin/fat interface and at its minimum at the skin surface. Then, a practical frequency of 5,8 GHz is selected once it belongs to the range of frequencies around the optimal one and ensures minimal interference with commercial communication systems in the industrial, scientific and medical (ISM) bands. Then, in order to demonstrate the effect of frequency on the standing wave pattern, a calculation of a plane wave travelling through a certain thickness skin layer and striking the skin/fat interface was conducted for different frequencies. At last, the electromagnetic fields were computed and utilised to determine the corresponding power absorption pattern which is expressed as the specific absorption rate.

Concerning the results of the specific absorption rate patterns, it can be observed that the absorption levels depends on the frequency. For lower frequencies, the absorption at the skin surface is much closer to the maximum absorption level at the skin/fat interface due to the longer wavelength. On the other hand, for higher frequencies, the wavelength in the skin diminishes

which, in turn, leads to a dual-peak response in which the maximum absorption level occurs at the skin/fat interface, as well as the skin surface.

With respect to results of preclinical trials, the ability of microwaves to target sweat glands depths in an efficient way was demonstrated, which led to the realisation of human trials. In human trials, the results were also positive once, through starch-iodine tests, a reduction in the secretion of sweat in the axilla was observed.

The commercial system described in this article contains a console and a handpiece. The console includes a 5,8 GHz power generator, a coolant pumping/chilling system, a vacuum system, a control hardware/software and a touchscreen user interface. The handpiece includes an antenna array, a cooling system and a temperature/power monitoring system [21].

2.2.2 Radio-frequency Based Therapeutic Approaches

2.2.2.1 Hyperthermia Treatment

The equipment presented in [22] is capable of preventing and control restenosis, which is a re-narrowing of blood vessels mainly due to scar-tissue proliferation within a stent, using an active stent targeted to endohyperthermia treatment in order to limit cell proliferation.

With regard to the design of the device, the active stent is constructed by electromechanically coupling an inductive stent with a planar capacitive element to establish an LC circuit that behaves as the wireless heater. This equipment is controlled using external RF fields that provide efficient RF-to-thermal energy conversion and high frequency selectivity, i.e., enables precision control of wireless thermal treatment while suppressing RF radiation power exposed to the body.

Regarding the operation, at a first stage the stent is implanted and expanded. Then, an AC current is generated when the circuit is exposed to an AC magnetic field which, in turn, is originated using a loop antenna aligned with the stent and connected to an RF signal generator through an amplifier. After that, the field power is converted to heating due Joule losses, resulting in the rise of the temperature that can be monitored using an infrared camera. The field power transferred to the circuit is maximized when the frequency of the external field matches the resonant frequency of the circuit, but this frequency changes as the device is implanted and expanded in a blood vessel due to the change in the inductance of the stent.

The process can be divided in three stages: device expansion, electromechanical characterisation and radio-frequency heating tests. The device expansion test refers to the stent expansion up to six millimetres in diameter by inflating the balloon catheter. After the deployment inside a silicone-based artery, it could be observed that the expansion process was made across the entire structure without any mechanical or electrical failure.

The electromechanical characterisation consists of studying the dependence of the device's resonant frequency on the radial size. For that purpose, the resonant frequency of the device was monitored while the expansion process occurred. By the analysis of the results, it was possible to verify that the resonant frequency shifted to lower levels as the expansion progressed because the larger the stent's diameter, the higher the inductance of the stent. Besides, the measured resonant

frequencies, i.e., 205.3 MHz and 145.6 MHz for, respectively, the unexpanded and fully expanded states, were very alike to the theoretical expected values, i.e., 213.8 MHz and 150.1 MHz for both cases [22].

In the heating tests, the radio-frequency magnetic fields were generated using a loop antenna aligned with the stent and connected to a radio-frequency signal generator through an amplifier. In order to monitor the device temperature, an infrared camera was used. At a first stage, the heating test was done with the unexpanded stent by radiating a radio-frequency field with a frequency equal to the resonant frequency (205.3 MHz) and output power of 320 mW. After that, a temperature increase with a maximum temperature of 57.7 °C was verified. On the other hand, for the expanded case, the radio-frequency output power was the same but the frequency was equal to the resonant frequency corresponding to the expanded device, 145.6 MHz. For that, a temperature increase of 63.8 °C could be observed. By the analysis of the results, it could be verified that the temperature was higher at the stent's center than in the stent's extremities and that a strong peak of temperature at the field frequency corresponding to the resonant frequency of the device which validated the frequency selectivity criteria [22].

Another example of a possible RF therapeutic approach is the TheraBionic therapy that has as main objective the treatment of inoperable liver cancer. This treatment uses a stainless steel antenna that transmits 27.12 MHz amplitude modulated radiation generated by an amplifier connected to the antenna.

Regarding the procedure, the patients need to place the antenna inside their mouths for a period of one hour and repeat it three times a day. During each treatment, the radio-frequency generator runs through 194 different modulations, which were determined by measuring variations of certain characteristics such as skin electrical resistance and pulse-amplitude, starting with 410 Hz until 21 kHz, each step lasting three seconds.

It is known that patients with liver tumours that cannot be completely removed during surgery have a small average survival time, about three to six months. With respect to the patients in this treatment group, the overall survival time was slightly greater, about six to seven months. However, for eight patients the survival time was much longer since they went on to live for more than two years. In four patients the size of the tumour decreased and some patients said that the pain disappeared or decreased after radio-frequency therapy [23].

A third example is the technique proposed by Hisanori Shoji [24] whose main goal is the treatment of advanced rectal cancer, based on a radio-frequency hyperthermia procedure for patients who were treated with preoperative hyperthermochemoradiation therapy. This study aimed at analysing the pathological and clinical response after eight weeks of treatment and also to evaluate the respective adverse effects.

This technique can be divided in two phases: a first stage where the patients are subject to radiation and, then, the hyperthermia process is realised using an 8 MHz RF capacitive heating device.

The chemo-radiation therapy was performed five times weekly and radio-frequency hyperthermia was realised once a week for five weeks, with fifty minutes irradiation. In the second method, the operator started from 200 W and the output was increased until complications such as pain appeared, being then decreased by 100 W, which was considered the optimal output dose without complications. Concerning the temperature measurement, a sensor catheter with four temperature points which provides the accumulated surface skin thermal output has been used.

Regarding the results' treatment, the average total accumulated irradiation output (TAIO) was proposed to be a quantitative parameter of the radio-frequency hyperthermia device that determines the output of this device while TATO was proposed to be the hypothetical heat dosage in patients. Concerning the temperature's results, it can be verified that temperature depends on individuals once certain individuals may be able to increase the set point of core temperature according to the output of radio-frequency irradiation.

With respect to side effects of hyperthermia, pain, unpleasant sensations, and burns could be observed in a small group of patients, due to the large reflections at the interfaces between soft tissue and bone or air. However, in most of cases, this treatment brought many benefits since adding radio-frequency hyperthermia has shown good local control and low toxicity [24].

2.2.2.2 Hyperthermia Treatment Using Sensitizers

Another example of the use of radio-frequency for therapeutic purposes is radio-frequency radiation-induced hyperthermia. This procedure can produce some side effects such as the heating of adjacent tissues, so it is necessary to have efficient biodegradable radio-frequency sensitizers in order to selectively target cancer cells.

This procedure was, previously, performed with gold nanoparticles but there are many disadvantages associated in the hyperthermia treatment. These include the fact that gold is not a biodegradable material and the injection of gold nanoparticles can lead to a long-term accumulation in the body with unclear consequences. Besides, these nanoparticles can hardly provide additional sensing, imaging or therapeutic functionalities.

In the method proposed by the authors [25], the process was performed with crystalline silicon based nanoparticles due to the many advantages of this type of material. These nanoparticles are biocompatible and biodegradable because, in biological tissue, they decay into orthosilicic acid which is excreted from the body through the urine. They also provide diagnostic and alternative modalities that can be applied in parallel to the radio-frequency hyperthermia treatment.

In first place, the sensitizers are targeted, actively (by using proper antibodies) or passively (by using the enhanced permeability and retention effect which is the natural capability of nanoparticles to preferably accumulate in tumours), into a tumour area and accumulated in it. The nanoparticles are then heated by RF radiation, resulting in a specific increase of temperature and precise death of cancer cells while the surrounding tissues remain unaffected, what can be explained by local currents in the electrical double layer near the surface of each nanoparticle. For the radio-frequency heating, a medical apparatus that provided electromagnetic radiation with frequency of 27 MHz and maximal power up to 66 W was used, providing a power source coupled to a pair

of electrodes with variable distance between them to measure the radio-frequency electrical field strength. The temperature of the nanoparticles was measured using an infrared thermometer after switching off the radio-frequency generator.

With the aim of studying the potential of these nanomaterials as sensitizers of radio-frequency induced cancer therapy, some in vitro and in vivo tests were made. From both tests it was possible to verify no toxicity issues that could affect the cell's proliferation and that these nanoparticles can serve as efficient sensitizers in this treatment, resulting in the inhibition of the tumour growth, as well as its elimination [25].

2.2.2.3 Tumour/Disease Ablation

The radio-frequency ablation method relies on electrical conduction through the tissues, i.e., an electrical circuit is created through the body. This current is capable of passing through tissues due to the abundance of ionic fluid. As tissues are not perfect conductors, electrical current causes resistive heating due to the Joule effect. This process results in the successful partial necrosis of the tumour being applicable only for a few organs such as liver, breast, lung, bone and kidney. Radio-frequency ablation is performed in the same way as the microwave ablation.

To successfully and predictably create an ablation requires the proper energy balance between the localized heating by the radio-frequency energy and the convected heating through the circulation of blood, lymph, or extra and intracellular fluid [20]. Approximately, the heat generated in a region at distance d from the heating source decreases as $1/d^4$.

The method presented in [26] allows for the controlled and direct destruction of the tumour using thermal or electrical energy. It is suited for patients who are high-risk surgical candidates with early stage lung cancer.

In radio-frequency ablation, with a frequency in the range of 460 to 480 kHz, an electrode is connected to a generator. The generator produces a voltage between the active electrode that is placed directly in the targeted tissue and the reference electrode. This voltage creates an electrical current capable of causing electron collisions with the adjacent molecules closer to the active electrode, producing heating of the target tissue from 60 °C to 100 °C. The temperature of the heated tissue is measured by the radio-frequency electrodes that have an internal thermocouple based temperature sensor. After the target tumour is treated, the radio-frequency electrode is removed.

In order to observe the success of the procedure it is necessary to apply certain techniques such as nodule CT densitometry and PET. Nodule CT densitometry helps to distinguish between more highly vascularised malignant nodules that enhance after contrast is administered. On the other hand, PET is useful due to the fact that radio-frequency ablation treated nodules have a significant decrease or absence of PET activity.

The possible side effects of this method are post-ablation syndrome, which is an inflammatory response, mild to moderate pain, mild pyrexia, pneumothorax, hemorrhage, damage to surrounding structures, skin burns resulting from inappropriate grounding pad placement, infection and abscess formation.

Regarding the antennas, which are straight applicators with active tips with various lengths, in both radio-frequency and microwave cases, it is necessary that they are internally cooled to reduce conductive heating and to prevent skin damage. The temperature can be measured with a separately placed thermocouple [26].

2.2.2.4 Tumour Ablation Using a Needle

This type of systems uses a high-frequency alternating electromagnetic field provided by induction coils, a magnetic material as a needle that can be influenced by the electromagnetic field, that when inserted into the target location can be heated up to a certain temperature capable of causing thermal ablation due to the presence of the electromagnetic field. However, the electromagnetic field has a limited effective range so for deep organ ablation it is necessary an electromagnetic thermotherapy system capable of inducing an efficient electromagnetic field.

This system consists of a synchronized-coil EMT system with an operating frequency of 58 kHz and power consumption of 25 kW for each generator, a two-section needle and a needle array insertion apparatus to control the arrangement of the needles and distance between them. The two-section needle includes a nonmagnetic section for contacting with the normal tissue and a magnetic section designed to be inserted into the target tissue. In order to improve the heating effect, two magnetic cores are placed on the top of the coils.

Regarding the experimental setup, it can be divided into four stages, the heating effect of the needle, the intensity of the electromagnetic fields, in vitro tests and in vivo animal tests.

The heating effect of the needle consists of the needle being heated up at the center of the synchronized coils by using four different kinds of induction coils (two-circle coils, surface coils, single-loop coils and the newly designed coils). This process lasts five minutes and the needle was heated up under the electromagnetic fields with ninety percent output power and the temperature distribution was measured. With respect to the results, it was possible to achieve that the temperature for the surface coils and the two-circle coils was not as higher as the other types of coils and that these two coils are not suitable for long distance minimally invasive surgery because the temperature is much lower when the distance between the coils is greater.

The second experience refers to the measurement of the intensity of the electromagnetic field without the magnetic core and with the magnetic core at different positions. From the results' analysis, it was verified that, by using simultaneously the E-magnetic core and the O-magnetic core, the intensity of the electromagnetic field increased and could be focused and that the position of the locally focused electromagnetic field could be controlled onto the target tissue to emphasise the treating effect.

In vitro tests were performed with porcine liver ex vivo by inserting the needle array under the electromagnetic thermotherapy system. Then, the needles were removed and the ablation area was

analysed on the porcine liver. Through the analysis of the ablation area, it could be observed that the needles placed in the effective electromagnetic field range were capable of being heated up to the specific temperature. Besides, this system could be used without the limitation of the treating area, because there was no needles' limit number, as long as they were placed inside the coils.

For the *in vivo* animal tests pigs were used and the two-section needle with a thermocouple was first inserted into the pig liver. Then, the needle array insertion apparatus was aligned with the temperature control monitoring needle, and the remaining two-section needles without thermocouples were placed around the last one. After the insertion, the needle array apparatus was removed and all two-section needles were heated to 98 °C for ten minutes, with an output power of 25 kW. After the treatment, the abdomen was incised and the ablation area on the liver was measured. After the surgery it was possible to verify, through the porcine liver, that there was no bleeding around the needle insertion hole which indicates that the blood vessels were successfully cauterised and that the normal tissue was not damaged [27].

2.2.3 Comparison Between Microwave Ablation and Radio-frequency Ablation

After comparing microwave ablation to radio-frequency ablation it is possible to identify many advantages and disadvantages of each one of these techniques.

As advantages microwave energy shows the fact that it is capable of propagating through materials with low or zero conductivity, the process of ablation is faster and high temperatures can be achieved. Microwave energy can also be used for multiple applicator ablation, i.e., multiple antennas can be operated continuously and simultaneously in close proximity or in separate locations, it offers more direct heating which is indicated for organs with high blood perfusion or near vascular heat sinks, and provides less procedural pain due to the lack of electrical stimulation associated with radio-frequency, and elimination of ground pad injuries. On the opposite side, microwave energy can overheat the cable used to transfer power from the generator to the applicator, so in order to counteract that the energy transmission is limited, an active cable cooling system is used to prevent thermal damage to normal tissues.

Radio-frequency ablation systems may be simpler and less costly to develop and are indicated for small volume thermal therapies once radio-frequency power deposition attenuates rapidly away from the radio-frequency electrode. As disadvantages radio-frequency ablation has a limited extent of induced necrosis or incomplete necrosis near blood vessels and the ablation zones do not exceed four centimetres unless ablation probe is repositioned for a second ablation [18], [28], [29].

Regarding the two methods, the choice of the most suitable ablation method depends on the tumour size. For tumours with diameters of three or less centimetres, both ablation methods can obtain good therapeutic effects, but radio-frequency ablation is more adequate once its electrodes can be adjusted to protect adjacent organs. On the other hand, for tumours with diameters greater than five centimetres, microwave ablation is the most suitable approach due to its higher intratumoural temperatures, larger tumour ablation volumes and shorter ablation times [30].

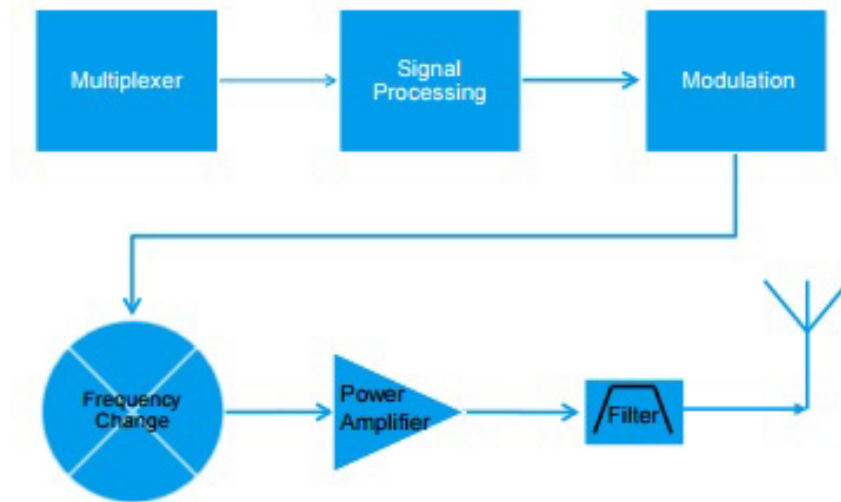


Figure 2.5: Block diagram of a simplified RF transmitter [5].

2.3 Radio-frequency Circuits

A basic RF system is composed by two parts, i.e., the transmission and the reception. It can be represented by the schematic diagrams shown in figures 2.5 and 2.6 that correspond, respectively, to a transmitter block diagram and a receiver block diagram.

A simplified RF transmitter comprises, firstly, a multiplexer, which is used to lead the desired information to the transmit path, and a signal processing stage in order to condition the signal for transmission. Then, the signal is modulated according to the application used being its frequency changed to the most suitable one for the particular application. A power amplifier is used to increase the signal level to the appropriate power level, a filter to ensure that the signal is maintained within the desired frequency band and the signal is, then, radiated through the air via an antenna [5].

In a simplified RF receiver the signal is received by the antenna and passes through a filter to extract the desired signal and, then, through an amplifier. After that, the frequency's signal is converted and the signal is demodulated, processed and conducted to the suitable signal path for the received information.

2.3.1 Power Amplifiers

In RF circuits, there are power amplifiers which are devices that receive an electrical signal and reprocess it to increase its power, i.e., increasing the input signal's voltage to obtain large power at the output.

The three main components of an power amplifier are the power supply, the input stage and the output stage. The power supply receives alternating current and converts it to direct current to send the DC signal to the input stage. Then, the signal is transferred to the output stage where it is amplified and converted to useful ac signal power [31], [32].

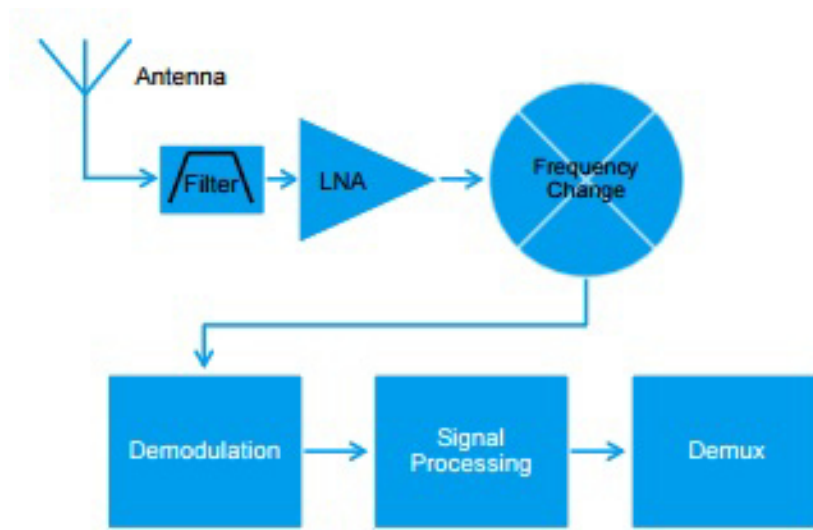


Figure 2.6: Block diagram of a simplified RF receiver [5].

In addition, power amplifiers can be separated in two groups: audio-power and radio-power amplifiers. For this particular case, radio-power amplifiers are the most suitable and are responsible for raising the power level of signals that belong to radio-frequency range, amplifying a specific frequency or narrow band of frequencies while rejecting all other frequencies, i.e., providing selectivity [32]. Power amplifiers can also be distinguished by class, i.e., can be characterised according to their circuit configuration and operation method. These amplifier classes represent the amount of the output signal that varies within the amplifier circuit over one cycle of operation when it is excited by a sinusoidal input signal [33].

Power amplifiers are specified in terms of power units known as Watt which is denominated as amplifier's power rating and reflects the maximum output that the power amplifier is capable of producing [32].

2.3.2 Impedance Matching

In RF circuits impedance matching is necessary to achieve maximum performance, i.e., to maximise the power transferred into the load or minimise the amount of power reflected back from the cable, or both.

In addition, if the cable and antenna or receiver impedances are not matched, some of the RF energy will not be transferred into the load, being instead reflected back along the cable, causing power loss and eventually cable damage and overheating [34]. The problem of mismatched load and source impedances can be corrected by using an impedance matching device between them, which can be a component or circuit [35].

However, the impedance matching is not always important, namely at the source end in the case of transmitters. Mismatching the impedance deliberately, i.e., having the transmitter impedance much lower than the input of the cable, can result in a decreasing of power lost in

the final stage and, also, ensure that if RF is reflected back from the antenna end, most of it is bounced right back again. In situations which impedance matching is performed at the source end of the cable, there is always a loss of power of 3 dB, because when the generator impedance and the impedance of its load are equal, half the power is lost in the resistance of the generator [34].

Related to impedance matching, there is the maximum power-transfer theorem that enunciates that to transfer the maximum amount of power from a source to a load, the source impedance should be equal to the load impedance. When this occurs, the amount of power delivered to the load is identical to the power dissipated in the source, which indicates that transfer of maximum power is only 50% efficient. To compensate this effect, the generator has to develop twice the desired output power [35].

2.3.3 Antennas

An antenna is a device capable of radiate and receive electromagnetic energy that can be considered resonant once operates efficiently over a narrow frequency band. Antennas can be classified according to the Voltage Standing Wave Ratio, the bandwidth and the directivity and the gain. The VSWR indicates the quality of the impedance matching, i.e., a high VSWR reports that the signal is reflected before being radiated by the antenna. On the other hand, the bandwidth is defined as function of VSWR or radiation patterns and can be calculated by the following equation:

$$B = \frac{F_H - F_L}{F_C}, \quad (2.14)$$

where F_H , F_L and F_C are the high, low and centre frequency of the band, respectively. The directivity is the ability of an antenna to focus energy in a certain direction when transmitting or vice-versa while the gain is considered the practical value of directivity and can be related to it by the next formula:

$$G = \eta \cdot D, \quad (2.15)$$

where G is the gain, D the directivity and η is a parameter that describes the antenna efficiency.

Related to antennas, there are radiation patterns whose function is the description of the relative strength of the radiated field in diverse directions at a constant distance. According to these, it is possible to distinguish the near-field, which refers to the field pattern present close to the antenna, and the far-field that is the field pattern at large distances.

There are many types of antennas such as wire-type antennas that are made of conducting wires and aperture-type antennas which are the most indicated to radiate and receive electromagnetic energy. For the desired case, i.e., radio-frequency hyperthermia treatment, the patch antenna, which is an example of aperture-type antennas, seems to be the most suitable once is capable of radiating only to one direction which is useful to target a certain tissue.

According to hyperthermia, antennas can be classified in invasive and non-invasive. Noninvasive antennas consist of E-type and H-type applicators. The first type produces electric fields capable of heating the tissue and operates at relatively low frequencies like 13,56 MHz though can

overheat the superficial and interfacing tissues. On the other hand, H-type applicators generate a magnetic field which, in turn, origins the electric field that heats the tissue and have as main advantage the fact that do not produce overheating of superficial and interfacing tissues. On the opposite side, there are invasive applicators that can heat in specific locations but are not adequate for all tumours [8].

2.4 Conclusions

From this chapter, it is important to note that radio-frequency and microwave radiation are considered non-ionizing radiations which can cause biological effects such as thermal effects, i.e., heating of biological tissues.

To study the interaction between electromagnetic fields and biological tissues it is necessary to have knowledge about the dielectric properties of the biological tissue subject to radiation. These properties are the electric conductivity, the electric permittivity and the magnetic permeability, and can be influenced by some factors such as frequency and temperature.

Concerning the effects of radiation on health, it is important to take in account that there is no relevant scientific evidence that indicates adverse health and biological effects as a result of radio-frequency exposure at lower levels than safety standards, not ensuring that exposure to weak electromagnetic fields is harmless to human body. However, the exposure to high levels of radio-frequency radiation can be prejudicial because that leads to the heating of biological tissue and respective increase of temperature. In turn, this could lead to tissue damage due to the body's inability to cope or dissipate the excessive heat, namely in areas with relative lack of available blood flow.

Regarding to electromagnetic radiation based therapeutic approaches, it is necessary to know that these can be separated in two groups according to the frequency range, microwave based therapeutic approaches and radio-frequency based therapeutic approaches. The use of each technique depends on some factors such as the type of condition/disease, the tumour size and even the dielectric properties of the specific tissues.

For the specific case of this work, which is the heating of biological tissues namely for hyperthermia treatment, it can be verified that for hyperthermia the most common frequency used is 27 MHz however 13,56 MHz is an optimal frequency for tissue heating due to the facility for radiation to propagate in biological tissues.

Chapter 3

An Electrical Model of Tissue Heating

The scenario being considered for the work developed in this dissertation is that of irradiating a body tissue with an external antenna. To know what power has to be irradiated to cause an increase of temperature ΔT in a specific part of the body, one needs to know the power loss occurring in the propagation path from the antenna to that body part and the power that needs to be dissipated in the specific tissue to be heated.

The tissue heating process is, in a very first approach a combination of power and time. Let's calculate the power needed to warm a mass of water from temperature T_1 to temperature T_2 in the period of time t seconds, is (IEC 60705 standard) given by equation 3.1,

$$P = \frac{4.187m_w(T_2 - T_1)}{t} + \frac{0.55m_c(T_2 - T_0)}{t}, \quad (3.1)$$

where 4.187 corresponds to the conversion of 1cal to Joule, m_w is the mass of water in grams, $T_2 - T_1$ the increase of temperature in °C. The second part of the equation concerns the heating of the water container. According to this calculation, a power of 7 mW (38,45 dBm) needs to be dissipated in each gram of water of a tumour, during 60 minutes, to increase its temperature from 36 °C to 42 °C.

On the other hand, let's calculate the power needed to heat up a tumour with a $1mm^3$, considering a heating time of 3600 seconds and an increasing in temperature of 6°C. Having in account a tumour with a $1mm^3$ the tumour mass is:

$$m_T = V \cdot \rho = 10^{-9}m^3 \cdot \frac{1050kg}{m^3} = 1.05mg \quad (3.2)$$

It is known that the deposited energy in the tumour can be calculated by the following equation:

$$\Delta Q = \Delta T \cdot C = \Delta T \cdot V \cdot \rho_T \cdot C_{pT} = 6^\circ C \cdot 10^{-9}m^3 \cdot \frac{1050kg}{m^3} \cdot 3852 \frac{J}{kg^\circ C} = 24.2mJ = 24.27mW \cdot s \quad (3.3)$$

It is also known that this energy corresponds to the needed energy to heat up $1mm^3$ tumor by

6°C and can be defined by the next equation:

$$\Delta Q = P \cdot \Delta t = \frac{24.27mW}{3600} = 6.74\mu W \quad (3.4)$$

So, it can be verified that the power per unit volume is:

$$P_V = \frac{\Delta Q}{V} = \frac{24.27mW \cdot s}{10^{-9}m^3} = 6741.7W/m^3, \quad (3.5)$$

where P_V is the power per unit volume.

In addition, the power per unit area is:

$$P_A = P_V \cdot Thickness = 6741.7 \frac{W}{m^3} \cdot 10^{-3}m = 6.7417W/m^2 \quad (3.6)$$

This value is considered the power dissipated needed to warm up the tumour and it is expressed by unit area, once the power dissipated obtained in ADS software only considers the thickness as geometric dimension. However, this calculation does not consider the occurrence of heat dissipation due to the fact of the tissue is not actually fully isolated from the surrounding tissues.

Electromagnetic thermal effects are commonly described by the Pennes' bio-heating equation 3.7 [36],

$$\nabla(-k\nabla T) = \rho_b C_b w_b (T_b - T) + Q_{met} + Q_{ext}, \quad (3.7)$$

where k is the tissue thermal conductivity (W/m⁰K), ρ_b is the blood density (kg/m³), C_b the blood specific heat (J/kg⁰K), w_b the blood perfusion rate (l/s)¹, T_b the blood temperature, and T the final temperature. Q_{met} is the energy source provided by the metabolism and Q_{ext} is the energy provided by an external source, i. e., the resistive heat generated by the electromagnetic field.

The electromagnetic heating process of a tissue is then a combined effect of two phenomena, the electric that concerns the field distribution, and the thermal connected with the temperature distribution. Considering a three-dimensional distribution of the electromagnetic field, the power (W/m³) inside the tissue volume can be described by equation 3.8 [37],

$$Q(x, y, z) = \frac{\sigma |\mathbf{E}(x, y, z)|^2}{2} = \frac{\sigma}{2} \left[\left(\frac{\delta \varphi(x, y, z)}{\delta x} \right)^2 + \left(\frac{\delta \varphi(x, y, z)}{\delta y} \right)^2 + \left(\frac{\delta \varphi(x, y, z)}{\delta z} \right)^2 \right], \quad (3.8)$$

This expression is similar to that seen for the SAR, considering now a 3-D form and using the tissue conductivity σ [S/m] instead of the tissue resistivity.

A 3-D form of the Pennes' equation becomes

$$-k\nabla^2 T(x, y, z) = \rho_b C_b w_b (T_b - T(x, y, z)) + Q_{met} + Q_{ext}(x, y, z), \quad (3.9)$$

¹The perfusion rate measures the blood flow through the capillaries per unit mass of tissue, expressed in millilitres per minute per 100 g — <http://medical-dictionary.thefreedictionary.com/perfusion+rate>

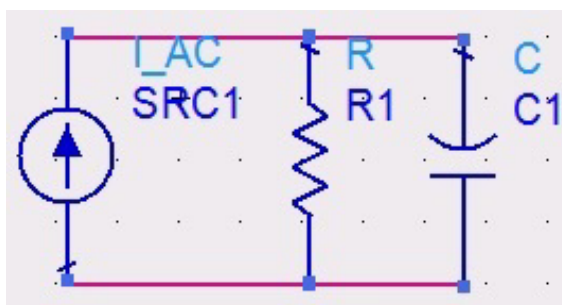


Figure 3.1: RC equivalent model of each tissue.

These models provide a means for the 3-D calculation of the electric field and temperature but are not useful to build a model where propagation through the different tissues is also included and which can be used in an electrical simulator such as the ADS (Advanced Design System) program.

3.1 Electrical RC Model of Biological Tissue

The objectives of developing a model for the power transmission process, given the wanted temperature rise and the depth of the spot to be heated, are:

- find the characteristics, power and frequency, of the radiation to be generated;
- determine the time needed to complete the tissue heating process;
- specify the characteristics to design the radiation emitting device.

In order to facilitate the development of this model, it is separated in two propagation paths, i. e., from the antenna through the air until the skin surface, and from the skin surface until the target tissue, being the equations for each case defined considering the different type of medium or tissues.

Consider that each tissue layer can be represented by the scheme in figure 3.1.

Having in account the RF propagation model, each tissue layer is represented by an RC circuit. From this specific case, three tissue layers were considered, skin, fat layer and breast tissue. For each tissue layer, it is necessary to determine the initial input power to be capable of calculating the power at a certain depth in the body. Then, with this value, it is possible to determine the power in a specific tissue at each unitary point to calculate the temperature rise in the tissue.

Since the skin surface includes capacitor C1, it is possible to deduce the current that passes through R1 (I_R) because in a resistance the current is in phase with the voltage while in a capacitor the current is lagged by 90° [38]. Therefore, it can be determined by the following equation:

$$I_R = I \cdot \sin \delta = I_{C1} \cdot \tan \delta, \quad (3.10)$$

where I is the current and δ is the loss angle.

Besides, the current in C1 is:

$$I_{C1} = \omega.V.C1 = 2\pi f.V.C1, \quad (3.11)$$

where ω is the angular frequency, V is the voltage applied at C1 and f is the frequency. So the current is:

$$I_R = 2\pi f.V.C1. \tan \delta \quad (3.12)$$

Therefore, the power can be determined by the following equation:

$$P_0 = \frac{V.I_R}{2} = \frac{V.2\pi f.V.C1. \tan \delta}{2} = \pi f.V^2.C1. \tan \delta \quad (3.13)$$

Then, assuming that C1 is a parallel plate capacitor and that can be represented by:

$$C1 = \epsilon_0.\epsilon''.\frac{S_1}{d_1} \quad (3.14)$$

where ϵ_0 is a constant, ϵ'' is the loss factor, S_1 is the plate area and d_1 is the plate separation. The power is:

$$P_0 = \pi f.V^2.\epsilon_0.\epsilon''.\frac{S_1}{d_1}. \tan \delta \quad (3.15)$$

Since

$$V^2 = E^2.d_1^2 \quad (3.16)$$

where E is the electric field strength. The power becomes then [39]:

$$P_0 = \pi f.E^2.\epsilon_0.\epsilon''.S_1.d_1. \tan \delta \quad (3.17)$$

The power, at a certain distance to the surface x , can be found by the equation:

$$P_x = P_0.e^{-2\alpha x}, \quad (3.18)$$

where α is the attenuation constant, which can be calculated for each tissue layer by the following equation:

$$\alpha = \frac{2\pi}{\lambda_0}.\sqrt{\frac{\epsilon''.\left(\sqrt{1 + \tan^2 \delta} - 1\right)}{2}} \quad (3.19)$$

where λ_0 is a constant [38].

Assuming each layer block as a cube with a face area S and edge length d , the power at each unitary area point can be obtained after dividing by $6d^2$. Therefore, the power for each unitary area point for any tissue can be represented by the equation:

$$P = \frac{P_0.e^{-2\alpha x}}{6d^2} \quad (3.20)$$

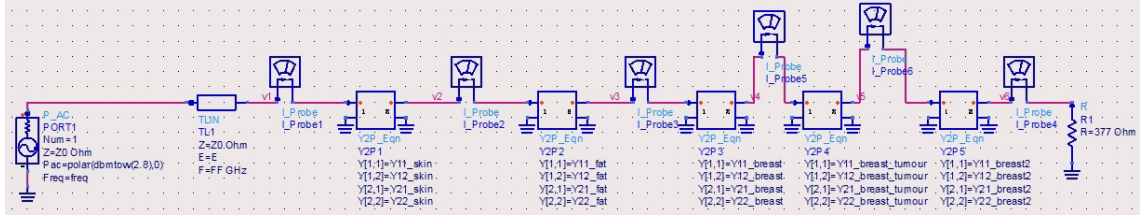


Figure 3.2: Representation of the electric circuit model used in the ADS.

where d and α are specific for each tissue.

After determining the power in the target tissue and knowing the heating time (Δt), it is possible to calculate the temperature rise that occurs within the heating process, according to the following equation:

$$\Delta T = \frac{\Delta t \cdot P_t}{C_p \cdot \rho} \quad (3.21)$$

where C_p is the specific heat, ρ is the density and P_t is the power in the target tissue [38].

3.2 Electrical Model Based on Electromagnetic Propagation

The following proposed model is being used to perform simulations with the Advanced Design System program. A new model was developed where each tissue layer is represented by a dipole, considering now the thickness of each layer namely 2 mm, 20 mm and 101 mm for skin, fat layer and breast tissue, respectively. The breast tissue is divided in three block whose thicknesses are, respectively, 30mm, 1mm and 70mm. The model used is represented in figure 3.2:

In this model, the different components correspond to a certain equipment or tissue. The power source corresponds to the antenna while the transmission line represents the propagation of radiation through air. In addition, the five dipoles correspond, respectively, to skin, fat layer, breast tissue, tumour and breast tissue.

Each tissue layer was defined by a set of variables that are represented in picture 3.3.

In first place, the propagation constant, which is represented by γ in ADS, is defined by the next equation, considering the equations 2.2, 2.3 and 2.4:

$$\gamma = \sqrt{j\omega\mu(\sigma + j\omega\epsilon')} = j\omega\sqrt{\mu\epsilon'} \cdot \sqrt{1 - j\frac{\sigma}{\omega\epsilon'}} \quad (3.22)$$

In addition, it is known that the voltage at each point can be calculated by the following equation:

$$V(z) = V_0^+ \cdot e^{-\gamma z} + V_0^- \cdot e^{\gamma z}, \quad (3.23)$$

where V_0^+ is the quantity of transmitted energy while V_0^- is the quantity of reflected energy. To represent this type of network it is more convenient to use a transmission matrix, i. e., the VAR4 in ADS, that relates the incident and reflected wave amplitudes on the input side of the network to

```

VAR
VAR1
Y11_tissue=YY_tissue*((1 - S11_tissue)*(1+S22_tissue)+S12_tissue*S21_tissue)/YD_tissue
Y22_tissue=YY_tissue*((1 + S11_tissue)*(1-S22_tissue)+S12_tissue*S21_tissue)/YD_tissue
Y12_tissue=YY_tissue*(-2*S12_tissue)/YD_tissue
Y21_tissue=YY_tissue*(-2*S12_tissue)/YD_tissue

VAR
VAR2
S11_tissue=A21_tissue/A11_tissue
S12_tissue=(A22_tissue*A11_tissue - A21_tissue*A12_tissue)/A11_tissue
S21_tissue=1/A11_tissue
S22_tissue=-A12_tissue/A11_tissue

VAR
VAR3
g_tissue=j*w*sqrt(uu*ee_tissue)*sqrt(1 -j*(cond_tissue/(w*ee_tissue)))
YD_tissue=(1 + S11_tissue)*(1 + S22_tissue)-S12_tissue*S21_tissue
YY_tissue=1/ZZ_tissue
ZZ_tissue=(j*w*uu)/g_tissue

VAR
VAR4
A11_tissue=exp(g_tissue*d_tissue)
A12_tissue=0
A21_tissue=0
A22_tissue=exp(-g_tissue*d_tissue)

VAR
VAR5
d_tissue=thickness
er_tissue=permittissue
ee_tissue=e0*er_tissue
cond_tissue=condtissue

```

Figure 3.3: Representation of the set of variables used in the electric circuit model.

those on the output side. So, the matrix $[A]$ was defined as shown in figure 3.4, considering that d is equal to the thickness of the tissue.

$$\begin{bmatrix} e^{\gamma d} & 0 \\ 0 & e^{-\gamma d} \end{bmatrix}.$$

Figure 3.4: Representation of the transmission matrix.

Then, it was possible to obtain the scattering matrix, which is represented by $[S]$ in ADS, that was calculated by the following equations:

$$S_{11} = \frac{A_{21}}{A_{11}} \quad (3.24)$$

$$S_{12} = \frac{A_{22}A_{11} - A_{21}A_{12}}{A_{11}} \quad (3.25)$$

$$S_{21} = \frac{1}{A_{11}} \quad (3.26)$$

$$S_{22} = \frac{-A_{12}}{A_{11}} \quad (3.27)$$

The obtained $[S]$ matrix is represented in figure 3.5.

$$\begin{bmatrix} S_{11} & S_{12} \\ S_{21} & S_{22} \end{bmatrix}.$$

Figure 3.5: Representation of the scattering matrix.

Table 3.1: Dielectric properties of each tissue for the different frequencies used in the simulated models [6].

Frequency (Hz)	Skin		Fat		Breast Gland	
	ϵ_r	σ (S/m)	ϵ_r	σ (S/m)	ϵ_r	σ (S/m)
13.56 M	2.85e2	2.38e-1	2.54e1	5.53e-2	1.32e2	7.29e-1
27.12 M	1.65e2	3.29e-1	1.79e1	6.10e-2	9.39e1	7.51e-1
433 M	4.61e1	7.02e-1	1.16e1	8.22e-2	6.13e1	8.86e-1
915 M	4.13e1	8.72e-1	1.13e1	1.10e-1	5.97e1	1.04
2 G	3.86e1	1.27	1.10e1	2.12e-1	5.78e1	1.63

In addition, the admittance matrix was defined by the following equations [40]:

$$Y_{11} = Y_0 \cdot \frac{(1 - S_{11})(1 + S_{22}) + S_{12}S_{21}}{(1 + S_{11})(1 + S_{22}) - S_{12}S_{21}} \quad (3.28)$$

$$Y_{12} = Y_0 \cdot \frac{-2S_{12}}{(1 + S_{11})(1 + S_{22}) - S_{12}S_{21}} \quad (3.29)$$

$$Y_{21} = Y_0 \cdot \frac{-2S_{21}}{(1 + S_{11})(1 + S_{22}) - S_{12}S_{21}} \quad (3.30)$$

$$Y_{22} = Y_0 \cdot \frac{(1 + S_{11})(1 - S_{22}) + S_{12}S_{21}}{(1 + S_{11})(1 + S_{22}) - S_{12}S_{21}} \quad (3.31)$$

Once admittance is the inverse of impedance, it was necessary to determine the intrinsic impedance of the tissue, which is calculated by the following equation [41]:

$$\eta = \frac{j\omega\mu}{\gamma} \quad (3.32)$$

With the aim of including the ISM frequencies for therapeutic/medical purposes, the frequency range chosen is from 10 MHz to 5 GHz. Due to the fact that the dielectric properties are frequency dependent, it was necessary to use a tissue database in order to determine the different values of the dielectric properties of each tissue in the frequency range and insert them into the software. From this tissue database it was possible to elaborate a table for each tissue that contains the electric permittivity and the electric conductivity for the respective frequency range. For the different simulated models, it was necessary to register the dielectric properties of each tissue for the different frequencies as shown in table 3.1 [6].

3.3 Thermal Models With Heat Dissipation

Having in account the equation 3.9, the evolution of temperature considers the absorbed energy, the heat dissipation by thermal conduction and heat dissipation through diffusion by bloodstream.

In these models, the energy source provided by the metabolism and the diffusion by bloodstream are not considered, it is only consider the dissipation through thermal conduction.

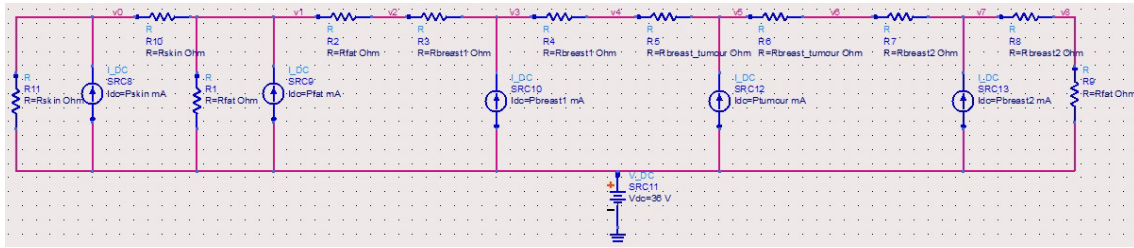


Figure 3.6: Thermal model with heat dissipation used in the ADS that simulates the temperature of the tumour.

In addition, since from the electrical model performed in ADS the values obtained for power dissipated are power per unit area due to the fact that the thickness is considered the only geometric dimension, it is necessary to multiply the values of power dissipated by area, i.e, 1mm^2 .

3.3.1 Stationary Thermal Model

In order to determine the temperature of the tumour when thermal equilibrium is established, the thermal model is extended considering a stationary model in which heat dissipation occurs as shown in figure 3.6.

For each tissue it was necessary to determine the respective thermal resistance using the following equation:

$$R_{th} = \frac{d}{k.S}, \quad (3.33)$$

where d is the tissue's thickness, k is the thermal conductivity and S is the section area. Since each tissue was considered to be heated from inside out, i. e., the tissue heats itself and the adjacent tissues, it was necessary to divide the respective thermal resistance by two.

In addition, each tissue was heated by a current source whose current value is equal to the power dissipated in this layer in the electrical model (3.2), considering that 1 W corresponds to 1 A. Therefore, the powers dissipated for each tissue were registered in the electrical model.

For this thermal model, the considered reference temperature is 36°C once it is the body temperature, and it is represented by a voltage source of 36 V.

3.3.2 Transient Thermal Model

In order to study the behaviour of temperature with time, a transient simulation was carried out for the ISM frequencies obtained from the model represented in the figure 3.6 and 2 GHz frequency to compare with experimental. For this model, the thermal capacity of each tissue is also considered, which is expressed in J/K and can be calculated by the following equation:

$$C = C_p \cdot \rho \cdot V, \quad (3.34)$$

where V is the tissue's volume.

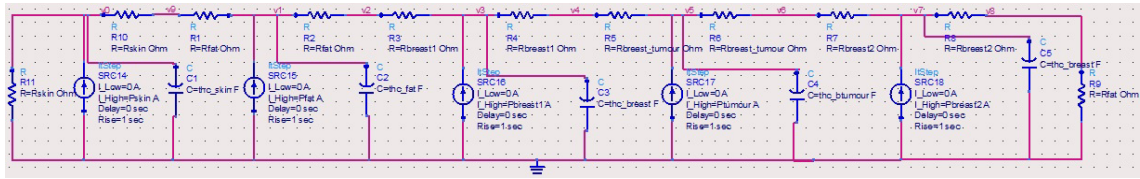


Figure 3.7: Transient thermal model with heat dissipation used in the ADS that simulates the behaviour of temperature through time.

The model used takes into account the thermal model with heat dissipation and is represented in figure 3.7.

A transient simulation was performed whose stop time was 3600 seconds and time step was 100 seconds.

Each tissue was heated by a step power (electric current) source whose value is equal to the power dissipated in this tissue. To measure the temperature variation in each tissue, a capacitor and a resistor are included that represent, respectively, the thermal capacity and thermal resistivity of the tissue, considering that $1 J/K$ corresponds to $1 F$ and $1 K/W$ to $1 Ohm$.

Also, to study the behaviour of temperature through time, the temperature increase was calculated by the next equation:

$$\Delta T = \frac{\Delta Q}{C}, \quad (3.35)$$

where ΔQ is the thermal energy and C is the thermal capacity. Since

$$\Delta Q = P.t, \quad (3.36)$$

the temperature variation can be determined by the following equation:

$$\Delta T = \frac{P_d.t}{C}, \quad (3.37)$$

where P_d is the power dissipated in the tissue and t is time.

3.4 Experimental

With the aim of studying the heating of tissues, a phantom (seen in picture 3.8) that represents breast tumour tissue, was prepared and placed near the antenna to be heated. The temperature was measured using an infrared thermometer camera with a thermal resolution of $0,068^\circ C$.

The materials used in the recipe used to create the phantom are presented in table 3.2.

Glycerine and sodium chloride were used to adjust both relative permittivity and conductivity. Agar was added to control the phantom's solidity [42].

The process to create the phantom is as follows:

1. Weigh all materials;
2. Heat water to $40^\circ C$;

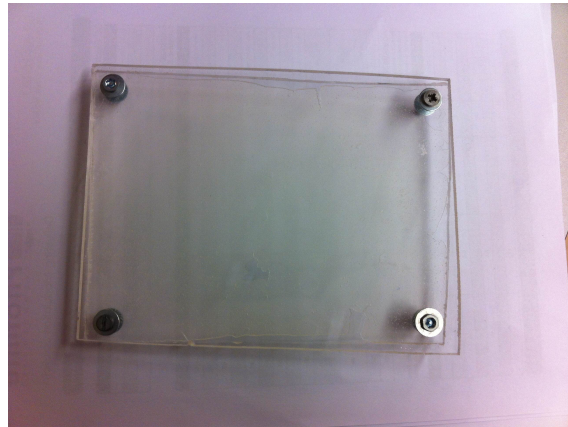


Figure 3.8: Phantom material that represents breast tumour.

3. Add all ingredients, mixing continuously;
4. Continue to stir at low speed to minimize the amount of air bubbles in the solution;
5. Remove from heat;
6. Continue to stir until mixture thickens;
7. Let cool to room temperature or place it in the fridge.

The scheme shown in figure 3.9 represents the setup implemented to perform the experimental evaluation.

This setup consists of a power source whose input power is -4 dBm and operates at a 2 GHz frequency. Then, two amplifiers were used whose gain is, respectively, 30 dBm and 15 dBm, and a wideband horn antenna, which has a gain of 9 dBi. While the antenna was irradiating the phantom the temperature was measured using the infrared camera. A metal plate was placed underneath the sample to ensure maximum electric field. In addition, since the phantom was placed between two acrylic plates to create a thin thickness, it was necessary to measure the temperature for a single acrylic plate to find out if it influenced the phantom heating. The material used in the experimental setup is presented in figures 3.10, 3.11, 3.12.

Table 3.2: Composition of breast tumour phantom.

Material	Tumour Phantom
Water	25 ml
Glycerine	15 ml
Silicone Emulsion	15 ml
Sodium Chloride	0.3 g
Agar	2.75 g

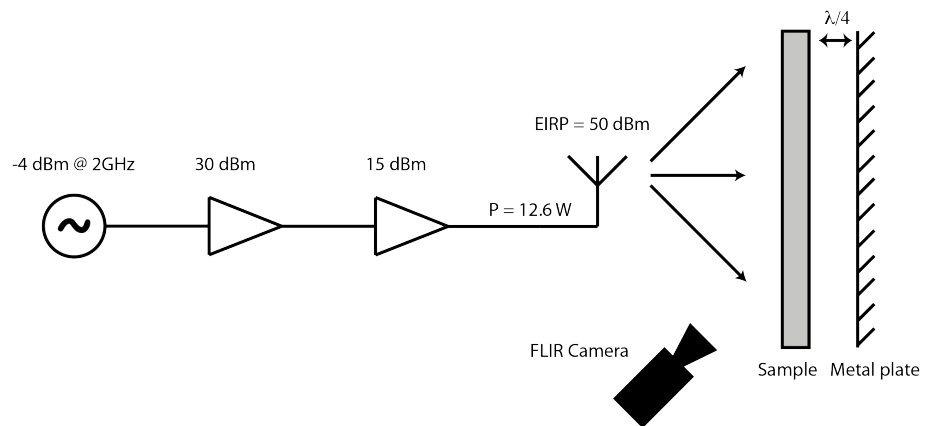


Figure 3.9: Scheme of the experimental setup used in the heating of the phantom.



Figure 3.10: Power source used in the experimental setup of the phantom heating.

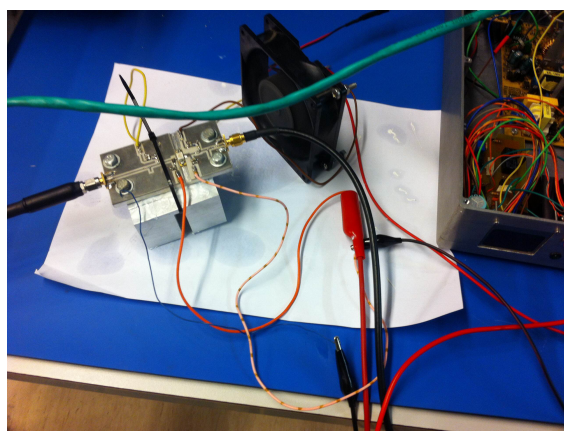


Figure 3.11: Amplifier used in the experimental setup of the phantom heating.

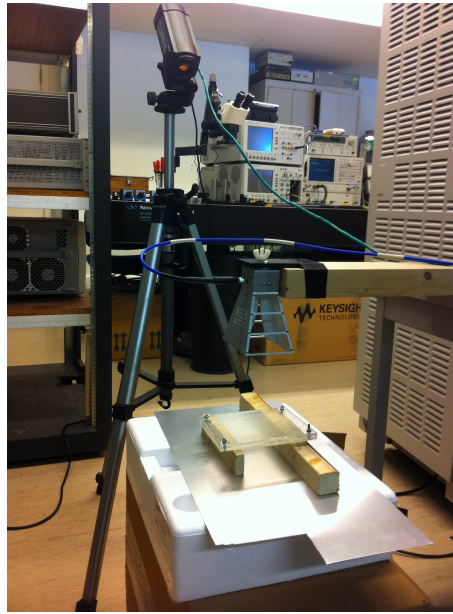


Figure 3.12: Antenna, phantom and camera used in the experimental setup of the phantom heating.

3.5 Conclusions

From this chapter, it is important to note that to simulate the heating of tissues, two approaches can be followed. The first approach is to determine the temperature of the tumour and the other tissues, considering stationary models without and with heat dissipation. The other approach is to consider a transient thermal model with heat dissipation in which the temperature rise of the different tissues is determined.

In addition, also to study the heating of tissues, experimental heating of tissues can be analysed to determine the temperature rise observed in the tumour by using a phantom that mimics breast tumour tissue and measuring its temperature with an infrared camera.

Chapter 4

Tissue Heating Simulation and Experimental Results

4.1 Simulations Results

4.1.1 Electric Model Based on Electromagnetic Propagation

Regarding the electric model and the respective frequency range chosen, simulations were performed to obtain the power dissipated in each tissue. The power values are expressed in % of the incident power in the tissue and were determined by the next equation:

$$P_d = \frac{P_i - P_o}{P_i}, \quad (4.1)$$

where P_i is the input power and P_o is the output power.

After running the simulation, it was possible to obtain these different values as shown in picture 4.1.

By the analysis of the graphic, it is possible to observe that the breast tissue has the highest power dissipated while the fat layer and skin present lower values for the power dissipated. In addition, the second layer of the breast tissue has the highest power dissipated while the tumour shows, along most of the simulation, a lower value for the power dissipated.

Comparing all types of tissue, the dielectric properties are different which can be considered as the reason for the differences observed between the powers dissipated. Taking into account the dielectric properties of each tissue, the fat layer has the lowest values for electric conductivity while the breast tissue has the highest and as frequency raises the electric conductivity increases as well, which can be seen in figure 4.2.

Therefore, relating the power dissipated with the electric conductivity, it appears that the higher the electric conductivity is, the higher the power dissipated in the tissue.

However, from approximately 2 GHz the fat layer presents a higher power dissipated compared to the skin, even with a lower conductivity, and the breast tumour, that has a slightly greater electric conductivity than the breast tissue, shows a lower power dissipated than the other layers of the

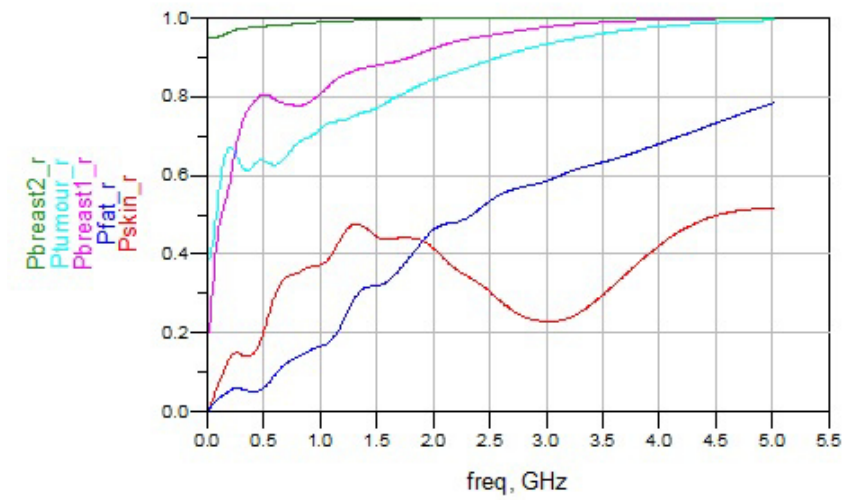


Figure 4.1: Representation of the power dissipated in each tissue as function of frequency.

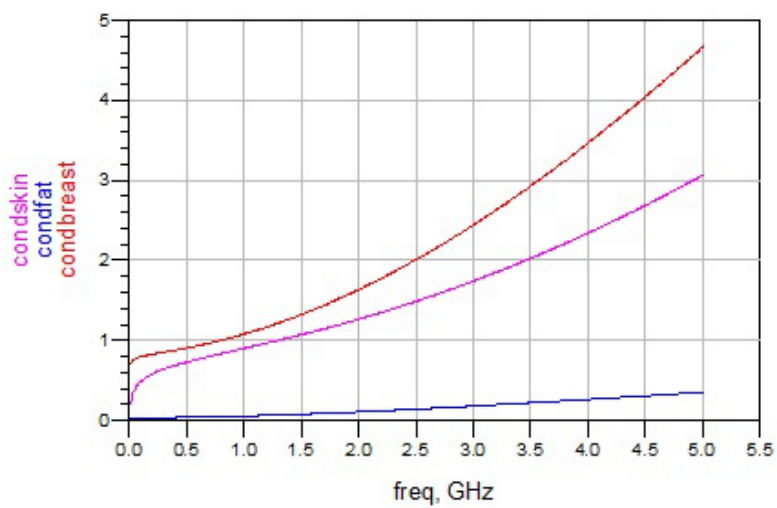


Figure 4.2: Representation of the electric conductivity in the tissues as function of frequency.

Table 4.1: Power dissipated in each tissue and voltage observed in the tumour for the different frequencies.

Frequency (Hz)	Pskin (W)	Pfat (W)	Pbreast1 (W)	Ptumour (W)	Pbreast2 (W)
13.56 M	0.215	0.293	10.730	1.672	25.397
27.12 M	0.543	0.390	11.688	1.674	24.711
433 M	34.099	9.179	95.495	6.637	33.865
915 M	114.395	30.290	116.796	6.313	27.470
2 G	49.156	31.422	33.768	0.718	2.067

breast tissue from approximately 240 MHz. These alterations could be justified by the differences in the thicknesses of the tissues.

Regarding the thicknesses, it can be seen that for greater thicknesses the power dissipated is higher, once the second layer of breast tissue has a 70 mm thickness and presents a higher dissipated power, compared to the first layer of breast tissue that has a 30 mm thickness and a lower power dissipated. Besides, the tumour layer presents a lower power dissipated even with a higher conductivity once it has a 1 mm thickness.

Taking into account the frequencies most commonly used for medical applications, the power dissipated in each tissue and the voltage observed in the tumour, i. e., v_4 , were determined in order to be used, respectively, in the thermal models with and without heat dissipation, for the different frequencies. The values are presented in table 4.1 and were obtained for an input power of 25 dBm.

From the various simulations, it is possible to deduce that for lower frequencies, such as 13.56 MHz and 27.12 MHz, the power dissipated in the first layers present lower values. On the other hand, for higher frequencies, such as 2 GHz, the power dissipated observed in the last layers are lower due to the fact that as frequency increases the penetration depth diminishes.

4.1.2 Thermal Models With Heat Dissipation

4.1.2.1 Stationary Thermal Model

After running the simulations, it was possible to determine these different values as shown in picture 4.3.

By the analysis of the picture 4.3, it can be seen that the achieved results are interesting once the temperatures obtained for the tumour are around the desired temperature increase which is around 40 °C. It is also possible to observe that for the adjacent layers of the tumour, the obtained temperatures are similar to the tumour's temperature. Since heat dissipation occurs it can be considered as the reason for these results, resulting in thermal equilibrium, i. e., when temperature stabilises.

Relating the values of the power dissipated in each tissue presented in table 4.1 with the obtained temperatures, it can be verified that, for most simulations, as power dissipated increases the temperature increases as well, as expectable. It can be also observed that the adjacent tissues influence the tumour's temperature since, for example, at 2 GHz the tumour presents the lower

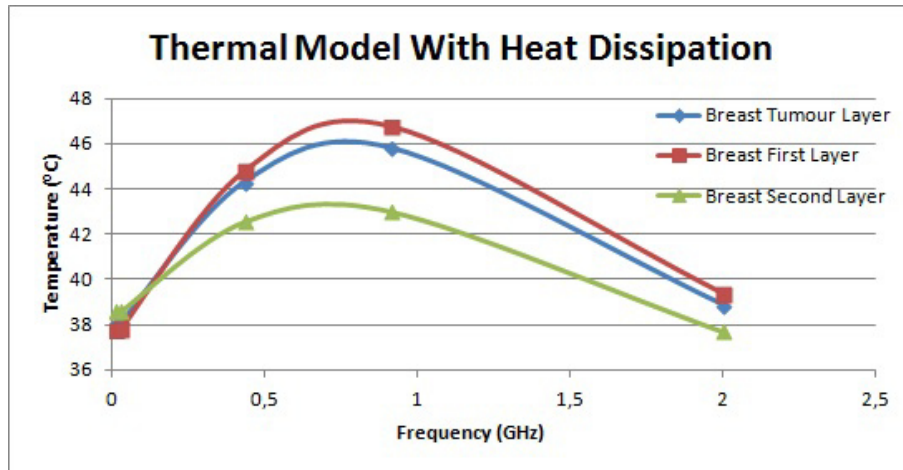


Figure 4.3: Temperature of the three layers of breast tissue at the different frequencies, for the thermal model with heat dissipation.

value for power dissipated but has a higher temperature compared to other frequencies such as 13.56 MHz and 27.12 MHz.

In addition, relating the obtained temperatures with frequency, it is possible to observe that the temperature increases until a maximum value at approximately 800 MHz and then decreases. Also, it can be seen that the most satisfactory temperature values are included in the frequency range from, approximately, 300 MHz to 1 GHz. Regarding this frequency range, two ISM frequencies can be identified, such as 433 MHz and 915 MHz.

Comparing the temperature of the tumour in both simulations, it is possible to observe that when heat dissipation was not considered, i.e., when an isolated tissue was considered, the temperatures were much higher than in the thermal model with heat dissipation, because the tissue was continuously heated. So, it can be verified that the temperature of the thermal model with heat dissipation corresponds to the limit temperature of the tumour, i.e., the temperature at which the thermal equilibrium is achieved.

4.1.2.2 Transient Thermal Model

The model was simulated for three frequencies 433 MHz, 915 MHz and 2 GHz, in which v0, v1, v3, v5 and v7 correspond to skin, fat, first layer of breast tissue, tumour and second layer of breast tissue, respectively. For 433 MHz it was possible to obtain the graphic presented in figure 4.4.

From the analysis of picture 4.4 it can be seen that the temperature increases with time. The temperature presents the lower values for skin and fat while the first layer of breast tissue and the tumour show the highest values for temperature. This difference can be explained by the higher volume of breast tissue and also for greater values of power dissipated. Despite the tumour shows a smaller volume, it presents a higher temperature due to the influence of the adjacent layers of breast tissue, which have higher values for power dissipated. In addition, considering that for an hyperthermia treatment a temperature increase of about 5 °C is necessary, it is possible to deduce

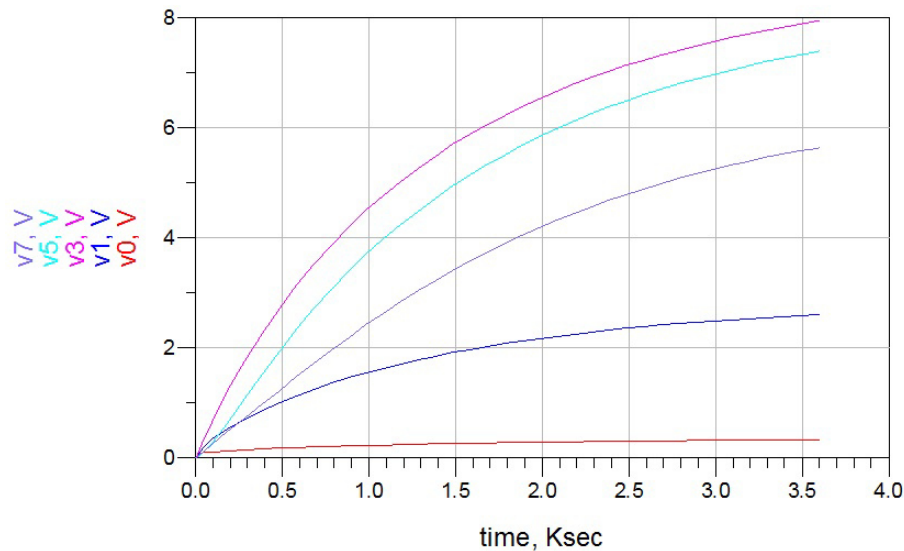


Figure 4.4: Variation of temperature through time for a frequency of 433 MHz.

that for achieving this temperature increase, a time of 1500 seconds, i. e., approximately, 25 minutes, is needed.

For 915 MHz, the graphic as shown in figure 4.5 was obtained .

From the analysis of picture 4.5, it can be verified that temperature also increases with time. The temperature presents the lower values for skin and fat, from approximately 1000 seconds, whereas the first layer of breast tissue and the tumour display the greater values of temperature. For the desired temperature increase, a time of about 1200 seconds is needed, i. e., approximately 20 minutes.

For 2 GHz, these different values were obtained as shown in picture 4.6.

After the analysis of the results, it is possible to observe that until, approximately, 1000 seconds the highest temperature belongs to the first layer of breast tissue and fat, but then the tumour presents a higher temperature increase. On the other hand, the second layer of breast tissue and skin show the lower temperature values due to the lower power dissipated.

Comparing the temperature rise in all simulations, it is possible to conclude that as power dissipated increases, the temperature rise increases as well, since for 2 GHz the maximum temperature rise for the tumour is approximately 2,5°C while for the others frequencies was, approximately, 8°C due to the higher values of power dissipated.

With respect to the temperature rise calculated in Excel through equation 3.37, was possible to obtain the graphic presented in figure 4.7.

From the analysis of figure 4.7, it can be verified that for the frequencies of 433 MHz and 915 MHz the obtained values are much greater than the values for 2 GHz, once for these frequencies the power dissipated in the tumour is much higher, leading to the conclusion that the temperature increase is directly proportional to the power dissipated in the tumour. Considering the desired temperature rise, about 5 °C, for 433 MHz and 915 MHz, heating times of 2900 seconds and 3200 seconds, i. e., 48 minutes and 53 minutes, are necessary, respectively.

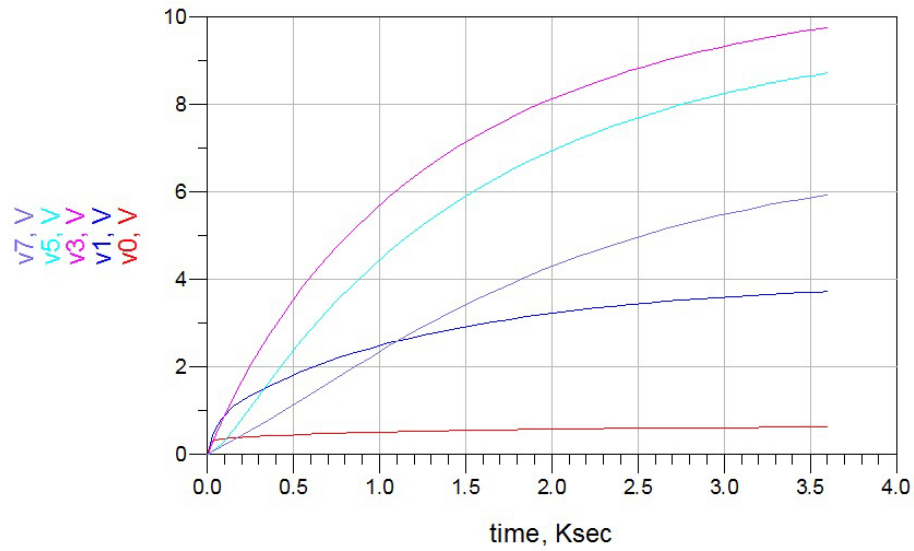


Figure 4.5: Variation of temperature through time for a frequency of 915 MHz.

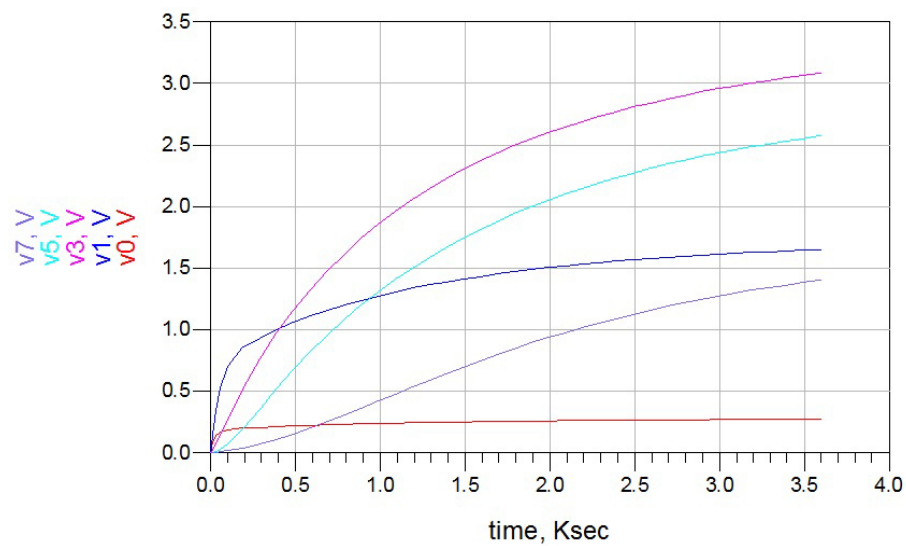


Figure 4.6: Variation of temperature with time for a frequency of 2 GHz.

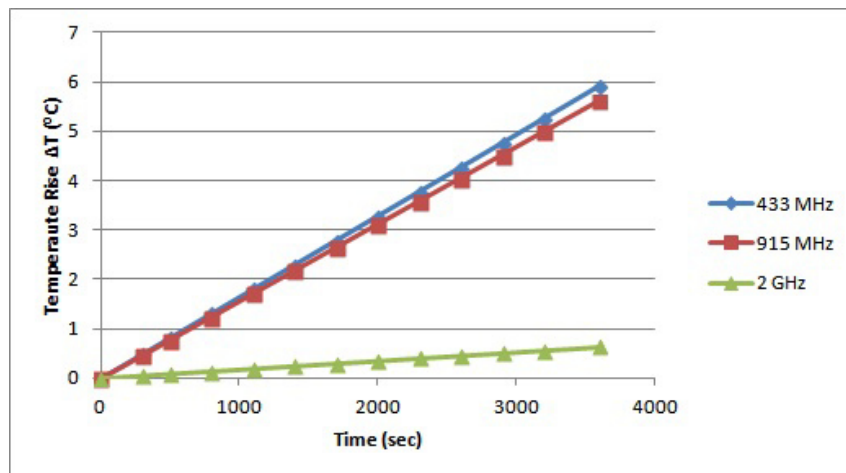


Figure 4.7: Variation of temperature with time for the different frequencies.

Comparing both results for the different frequencies, it can be seen that the temperature increase in simulations is higher than that obtained from equations 3.35 and 3.37. The fact that in the simulations all tissues in the heating process were considered, can be the reason for this difference, because the adjacent tissues of the tumour are capable of influencing the temperature rise in the tumour. To achieve the desired temperature increase, for simulations performed in ADS, the time needed is much lower, compared to the time obtained from the numerical results, once in the last method the other tissues were not considered. In addition, it is possible to verify that the calculated results are similar to the simulated results.

4.2 Experimental Results

With respect to the experience, the exposure time was, approximately, 20 minutes for each trial, i.e., for the phantom heating and for the heating of the acrylic plate. In order to observe the evolution of temperature, the first and last frames were saved for each experience, which are presented below.

As for the phantom heating, the figures 4.8 and 4.9 were obtained.

For the heating of the acrylic plate the results obtained are presented in figures 4.10 and 4.11.

Concerning figures 4.8 and 4.9, it can be seen that there is an increasing in temperature of, approximately, 1,5°C, since the initial temperature was near 25°C and the final temperature was 26,5°C. This temperature rise was not as high as desired once the temperature in the room is variable. In addition, the phantom was not heated equally which might have happened due to the fact that in the borders the thickness of the phantom was lower which leads to an easier heating.

On the other hand, regarding figures 4.10 and 4.10, it is possible to observe that the acrylic plate was not heated and the temperature was kept constant. So comparing both experiences, it is possible to conclude that the acrylic plates did not influence the heating of the phantom.

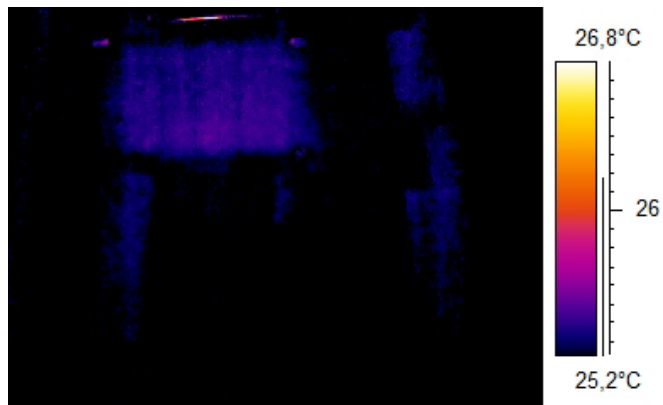


Figure 4.8: Phantom at the beginning of the exposure time.

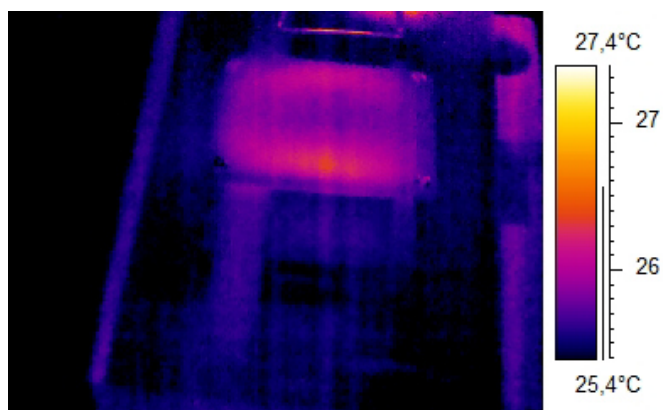


Figure 4.9: Phantom at the end of the exposure time.



Figure 4.10: Acrylic plate at the beginning of the exposure time.

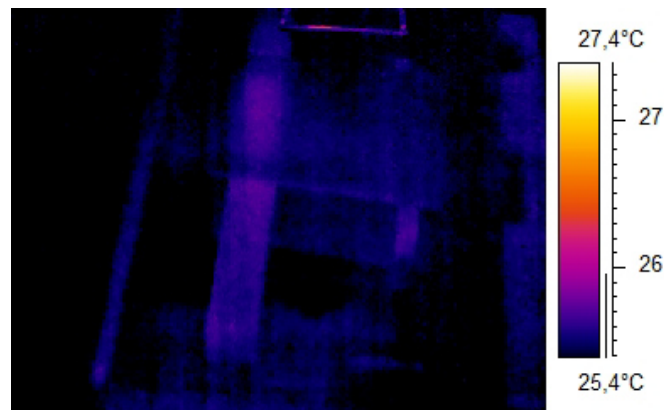


Figure 4.11: Acrylic plate at the end of the exposure time.

4.3 Conclusions

From this chapter, it is important to note that the temperature can be influenced by different factors.

With regard to the thermal model presented in the figure 3.6, it can be observed that the obtained values are interesting once the temperatures obtained for the tumour are around the desired temperature increase which is around 42°C. Besides, the temperatures of the adjacent layers of the tumour are similar to the tumour's temperature and that they are capable of influencing the tumour. In addition, the temperature of the tumour is directly proportional to the power dissipated, as expectable. In addition, the temperature obtained in the thermal model with heat dissipation is the limit temperature that the tumour achieves.

From the transient thermal model, it can be seen that the temperature increases with time and to achieve the desired temperature increase, for 433 MHz and 915 MHz frequencies, a time of, approximately, 22 minutes is needed.

With respect to experimental results, it is possible to verify that there is an increasing in temperature of, approximately, 1.5 °C. This temperature rise is not as high as desired, because the room's temperature is variable.

Comparing the temperature rise obtained in the simulations and in experimental trials, it can be verified that the increasing in temperature is higher in simulations once there are no losses in this process.

Chapter 5

Conclusions and Future Work

With respect to the goals of this dissertation, it is possible to conclude that the heating of tissues could be verified by the analysis of the simulations and experimental results.

Through simulations, the temperature of the tissues for stationary thermal model with heat dissipation was determined. In simulations, the temperature rise after the heating process was also obtained, using a transient thermal model with heat dissipation. After running simulations, it can be seen that the results obtained for the tumour's temperature and the temperature rise were satisfactory, because they are similar to the values used in the current therapies. In addition, it is possible to see that the values for tissue's temperatures and temperature rise obtained are similar.

On the other hand, through experimental trials, the heating of a tumour was verified using a breast tumour emulating phantom placed between two acrylic plates. By the analysis of the experimental results, it was possible to verify that the temperature rise observed was not as high as desired and that the acrylic plates do not influence the phantom heating. To counteract these results, i. e., to achieve a greater temperature rise, the experience should be done in a more constant environment in order to avoid temperature changes in the room.

Comparing both results, it is possible to conclude that the temperature rise in the simulations is higher, once there are no losses in the path due to the fact that ideal transmission lines are used and the input power is totally absorbed by the human body simulation model.

In addition, for the different simulations done in ADS, the heat dissipation through diffusion by bloodstream is not considered which can lead to minor values for tumour's temperature and temperature rise.

5.1 Future Work

With the aim of improving the obtained results, it is possible to do some different perspectives of work.

To consider heat dissipation through diffusion by bloodstream and through thermal conduction, it can be included the diffusion by bloodstream in this model version.

To avoid changes in the temperature of the environment medium, i. e., to ensure that the environment temperature is kept constant, the experience can be done in a reverberation chamber.

Another possible solution is to use an array of antennas to focus the radiation and irradiate more efficiently to the desired point.

To test for different frequencies, a wideband antenna or various antennas corresponding to the frequencies chosen can be used .

In addition, it could be interesting, in order to study the heating of different tissues at the same time, to use a multilayer phantom or more phantoms corresponding each one to a specific tissue.

References

- [1] M. Contents. (2016, Jul.) Electromagnetic spectrum. [Online]. Available: <http://www2.lbl.gov/MicroWorlds/ALSTool/EMSpec/EMSpec2.html>
- [2] S. of Biological Science. Types of tissues. [Online]. Available: <http://tmfpff.blogspot.pt/2011/06/tissue.html>
- [3] P. heating technologies. Induction heating. [Online]. Available: <http://www.thehomelaundrycompany.co.uk/petrield.com/index.php/Induction>
- [4] J. M. Felício, C. A. Fernandes, and J. R. Costa, “Microwave imaging for target detection in body phantom using the kirchoff migration algorithm,” *Antennas and Propagation Group*, 2013.
- [5] N. Jarvis, “Introduction to rf design,” in *Introduction to RF Design*, R. . Schwarz, Ed., 2014.
- [6] Z. MedTech. Tissue frequency chart. [Online]. Available: <http://www.itis.ethz.ch/virtual-population/tissueproperties/database/tissue-frequency-chart/>.
- [7] J.-P. Andretzko, “Contribution à l’optimisation et à la modélisation d’un banc de mesure cem-application à la caractérisation de l’immunité des stimulateurs cardiaques,” Ph.D. dissertation, Université Henri Poincaré-Nancy I, 2007.
- [8] Y. Huang and K. Boyle, *Antennas: from theory to practice*. John Wiley & Sons, 2008.
- [9] C. Meola, A. Christophe, G. M. Carlomagno, G. Klaus, G. Ermanno, K. Ivana, K. Petr, M. Carosena, P. Rocco, R. Roberto *et al.*, *Infrared thermography recent advances and future trends*, 2012.
- [10] W. H. Organization. What are electromagnetic fields? [Online]. Available: <http://www.who.int/peh-emf/about/WhatisEMF/en/index1.html>
- [11] C.-K. Chou, G.-W. Chen, A. W. Guy, and K. H. Luk, “Formulas for preparing phantom muscle tissue at various radiofrequencies,” *Bioelectromagnetics*, vol. 5, no. 4, pp. 435–441, 1984.
- [12] J. Flores, J. Becerra, and P. L. Ramírez, “Study on the transmission of an rf signal through phantom muscle tissue,” *International Journal of Advanced Research in Computer and Communication Engineering*, vol. Vol. 1, 2012.
- [13] Z. Pšenáková and V. PŠENÁK, “Electromagnetic heating of human tissue,” *Acta Mechanica Slovaca YBERC*, pp. 209–214, 2005.
- [14] M. Karunaratna and L. Dayawansa, “Energy absorption by the human body from rf and microwave emissions in sri lanka,” *Sri Lankan Journal of Physics*, vol. 7, 2006.

- [15] E. Pirogova, I. Cosic, and V. Vojisavljevic, *Biological effects of electromagnetic radiation*. INTECH open Access Publisher, 2009.
- [16] E. Committee, “Low-level radiofrequency electromagnetic fields – an assessment of health risks and evaluation of regulatory practice,” Norwegian Institute of Public Health, Tech. Rep., 2012.
- [17] C. on Assessment of the Possible Health Effects of Ground Wave Emergency Network, *Assessment of the Possible Health Effects of Ground Wave Emergency Network*. The National Academies, 1993.
- [18] C. L. Brace, “Radiofrequency and microwave ablation of the liver, lung, kidney, and bone: what are the differences?” *Current problems in diagnostic radiology*, vol. 38, no. 3, pp. 135–143, 2009.
- [19] S. Goldberg and G. Gazelle, “Radiofrequency tissue ablation: physical principles and techniques for increasing coagulation necrosis,” *Hepatogastroenterology*, vol. 48, no. 38, pp. 359–367, 2001.
- [20] C. J. Simon, D. E. Dupuy, and W. W. Mayo-Smith, “Microwave Ablation: Principles and Applications,” *RadioGraphics*, vol. 25, no. Suppl 1, pp. S69 – S83, 2005.
- [21] J. E. Johnson and S. Kim, “Dont sweat it: Treating hyperhidrosis with microwaves,” *Microwave Magazine, IEEE*, vol. 16, no. 2, pp. 31–38, 2015.
- [22] Y. Luo, M. Dahmardeh, X. Chen, and K. Takahata, “Selective rf heating of resonant stent toward wireless endohyperthermia for restenosis inhibition,” in *Micro Electro Mechanical Systems (MEMS), 2014 IEEE 27th International Conference on*. IEEE, 2014, pp. 877–880.
- [23] M. News. (2011, aug) Very weak rf signals show promise for treating inoperable liver cancer. [Online]. Available: <http://microwavenews.com/HCC.html>
- [24] H. Shoji, M. Motegi, K. Osawa, N. Okonogi, A. Okazaki, Y. Andou, T. Asao, H. Kuwano, T. Takahashi, and K. Ogoshi, “A novel strategy of radiofrequency hyperthermia (neothermia) in combination with preoperative chemoradiotherapy for the treatment of advanced rectal cancer: a pilot study,” *Cancer medicine*, vol. 4, no. 6, pp. 834–843, 2015.
- [25] K. P. Tamarov, L. A. Osminkina, S. V. Zinovyev, K. A. Maximova, J. V. Kargina, M. B. Gongalsky, Y. Ryabchikov, A. Al-Kattan, A. P. Sviridov, M. Sentis *et al.*, “Radio frequency radiation-induced hyperthermia using si nanoparticle-based sensitizers for mild cancer therapy,” *Scientific reports*, vol. 4, p. 7034, 2014.
- [26] E. S. Alexander and D. E. Dupuy, “Lung cancer ablation: technologies and techniques,” in *Seminars in interventional radiology*, vol. 30, no. 2. Thieme Medical Publishers, 2013, p. 141.
- [27] S.-C. Huang, J.-W. Kang, H.-W. Tsai, Y.-S. Shan, X.-Z. Lin, and G.-B. Lee, “Electromagnetic thermotherapy for deep organ ablation by using a needle array under a synchronized-coil system,” *Biomedical Engineering, IEEE Transactions on*, vol. 61, no. 11, pp. 2733–2739, 2014.
- [28] C. Chou, “Radiofrequency hyperthermia in cancer therapy,” *Chapter 94In Biologic Effects of Nonionizing Electromagnetic Fields, CRC Press, Inc*, pp. 1424–1428, 1995.

- [29] C. L. Brace, “Microwave tissue ablation: biophysics, technology, and applications,” *Critical ReviewsTM in Biomedical Engineering*, vol. 38, no. 1, 2010.
- [30] X. Ye, W. Fan, J.-h. Chen, W.-j. Feng, S.-z. Gu, Y. Han, G.-h. Huang, G.-y. Lei, X.-g. Li, Y.-l. Li *et al.*, “Chinese expert consensus workshop report: Guidelines for thermal ablation of primary and metastatic lung tumors,” *Thoracic Cancer*, vol. 6, no. 1, pp. 112–121, 2015.
- [31] wiseGEEK. What is a power amplifier? [Online]. Available: <http://www.wisegeek.com/what-is-a-power-amplifier.htm>
- [32] C. Today. (2009, sep) Power amplifiers and various types. [Online]. Available: <http://www.circuitstoday.com/power-amplifiers>
- [33] B. E. Tutorials. (2016) Amplifier classes. [Online]. Available: <http://www.electronics-tutorials.ws/amplifier/amplifier-classes.html>
- [34] J. Electronics, “Impedance matching: a primer,” *Jaycar Electronics*, 2001.
- [35] E. Design. (2011, oct) Back to basics: Impedance matching (part 1). [Online]. Available: <http://electronicdesign.com/communications/back-basics-impedance-matching-part-1>
- [36] M. F. J. C. Rubio, A. V. Hernández, and L. L. Salas, “High temperature hyperthermia in breast cancer treatment,” in *Hyperthermia*, N. Huilgol, Ed. InTech, 2013, ch. 2, pp. 83–100.
- [37] M. P. Ewa Majchrzak, “Numerical modelling of tissue heating by means of the electromagnetic field,” *Scientific Research of the Institute of Mathematics and Computer Science*, vol. 9, no. 1, pp. 89–97, 2010.
- [38] M. Orfeuill, *Électrothermie Industrielle*. dunod, 1981.
- [39] F. Marra, L. Zhang, and J. G. Lyng, “Radio frequency treatment of foods: Review of recent advances,” *Journal of Food Engineering*, vol. 91, no. 4, pp. 497–508, 2009.
- [40] H. J. Visser, “Appendix e: Two-port network parameters,” *Antenna Theory and Applications*, pp. 245–247.
- [41] M. inês Barbosa de Carvalho. (2005, oct) Guias de ondas. [Online]. Available: https://web.fe.up.pt/~hsalgado/ETeorica/docs/guias_v2.pdf
- [42] F. Komori, S. Kato, and T. Maeda, “x2 scale breast phantom for reproducing human breast cancer tissue,” in *Antennas and Propagation (ISAP), 2012 International Symposium on*. IEEE, 2012, pp. 1100–1103.